AN ANALOG ELECTRO-OPTICAL MULTIPLIER

by

Thomas M. Anderson

Electronic Systems Laboratory

MASSACHUSETTS INSTITUTE OF TECHNOLOGY, CAMBRIDGE 39, MASSACHUSETTS

Department of Electrical Engineering

AN ANALOG ELECTRO-OPTICAL MULTIPLIER

by

THOMAS M. ANDERSON

B. S. United States Naval Academy
(1960)

SUBMITTED IN PARTIAL FULFILLMENT OF THE
REQUIREMENTS FOR THE DEGREE OF
MASTER OF SCIENCE

at the

MASSACHUSETTS INSTITUTE OF TECHNOLOGY
September, 1963

AN ANALOG ELECTRO-OPTICAL MULTIPLIER

by

Thomas M. Anderson

Submitted to the Department of Electrical Engineering on September 27, 1963 in partial fulfillment of the requirements for the degree of Master of Science.

ABSTRACT

An Analog Electro-Optical Multiplier, a simple and compact solid state device with no moving parts, has been designed, constructed, and tested. Functionally, this device is the direct analog of the familiar servo-multiplier, being capable of multiplying one analog variable by up to seven other individual analog variables. The servo-driven potentiometer arm has been replaced by a photoconductive cell, illuminated by a low-power lamp, connected in a bridge circuit with two fixed resistors. The servomechanism driving the potentiometer arm has been replaced by a solid state operational amplifier driving the lamp in response to the value of the multiplicand.

Accuracies of 0.62 per cent of full scale have been obtained with this multiplier which has a dynamic range of 4 cps. An important advantage of this multiplier is the appreciable reduction in the number of operational amplifiers required compared to analog multipliers currently on the market, both for four quadrant and two quadrant multiplication.

Initial experiments were conducted using the Raytheon Raysistor, an electro-optical device consisting of a light source and a CdSe photoconductive cell. The effects of signal heating, hysteresis, and signal voltage across these cells is discussed and compared with the improved characteristics of the CdS photocells which were used in the final design.

The problem of uniformly illuminating several of these cells with a single lamp is discussed. In addition, the properties of miniature lamps with regard to light output, power requirements, and speed of response is considered.

ACKNOWLEDGEMENTS

The Analog Electro-Optical Multiplier was conceived by Mark E. Connelly, a project engineer at the Electronic Systems Laboratory, Massachusetts Institute of Technology. The author thanks him not only for providing an interesting and practical thesis topic, but also for his constant encouragement and helpful advice.

The laboratory machine shop personnel deserve a commendation for a job well and rapidly done, and the fine performance of the drawing room staff, especially Norman Darling who helped to design the lamp-photocell package and Harold Tonsing head of the department, is very much appreciated.

Thanks are also extended to Mr. Alfred K. Susskind, Associate Professor of Electrical Engineering for directing the author to a suitable topic and for acting as his faculty thesis supervisor, and to Norma Calder who typed this thesis.

This work was sponsored by the Aerospace Medical Division of the U. S. Air Force under contract number AF-33(616)-8363, DSR contract 8823.

TABLE OF CONTENTS

LIST OF FIGURES

List of Figures (cont)

CHAPTER I

INTRODUCTION

A majority of the devices used for the multiplication of two variables may be generally described by a block diagram such as the one shown in Fig. 1-1. The transfer function of this device is seen to be

$$K(X) = \frac{Z}{Y}$$

where $K(X)$ is a function of the input X to the multiplier. Thus Y is multiplied by a quantity which is proportional to X in order to obtain Z. Although many methods of multiplication by mechanical, electronic, electromechanical, and thermal means have been devised with varying degrees of success, the most frequently employed types for d-c analog computers are servo-driven potentiometers, time division multipliers, and the quarter square multiplier.

A typical servomultiplier is shown in Fig. 1-2. Inputs $+Y$ and $-Y$ are applied to the ends of the linear potentiometer. If the potentiometer setting is made proportional to the second input voltage, X, then the output voltage must be proportional to the product $Z = XY$. A servomechanism consisting of an amplifier and an electric motor can be made to position the potentiometer shaft in the desired manner. The voltage X is applied to the input terminal of the servomechanism, and the servomotor turns the shaft continuously to the correct setting. Note that a single servomechanism can multiply each of several machine variables by a function of the servo input

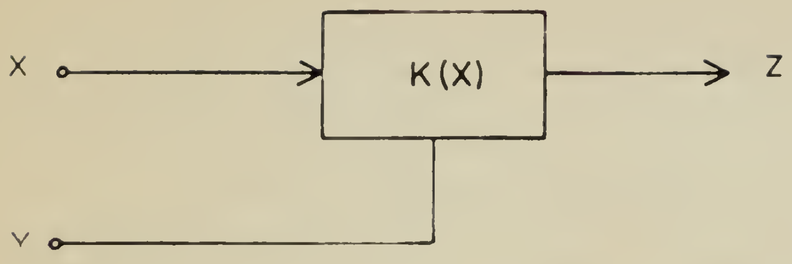

Fig. 1-1: GENERAL BLOCK DIAGRAM OF A MULTIPLIER

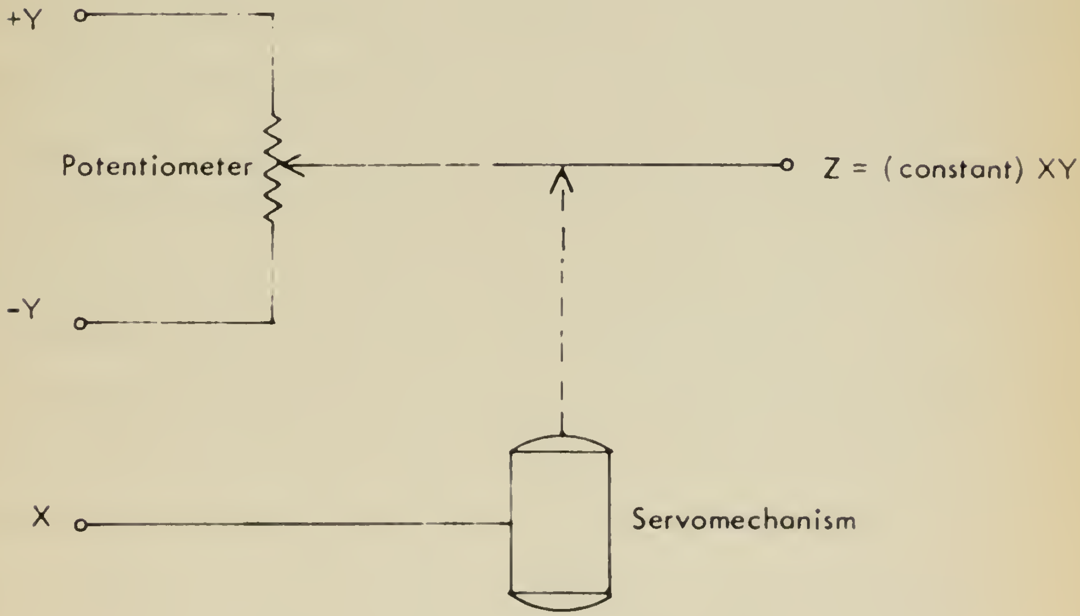

Fig. 1-2: SERVOMULTIPLIER

voltage. Accuracies better than 0.1 per cent have been attained with this type of multiplier. However, the frequency range of the "slow" variable is limited to 10 cps or less.[1*]

Of the two all-electronic multipliers mentioned, the quarter-square is less expensive and therefore more commonly used. The device makes use of the relationship

$$XY = \frac{1}{4} \left[(X+Y)^2 - (X-Y)^2\right]$$

in order to compute the required product. This has been done by using diode-resistance networks to form piecewise-linear parabolic characteristics, or by using the quadratic relation between grid voltage and plate current of a special tube. These two schemes utilize four squaring devices and three operational amplifiers to perform 4-quadrant multiplication illustrated by the block diagrams in Fig. 1-3(a). The use of absolute magnitude circuits reduces equipment requirements to two squaring circuits and two operational amplifiers as shown in Fig. 1-3(b). In some commercial quarter-square multipliers, these functions have been combined in a passive diode-resistance network which requires only ±X and ±Y signal inputs. Since the output is available as a current for all of the above schemes, an additional operational amplifier is required to transform the current to a voltage if a low impedance source is needed. Accuracies of better than 0.2 per cent at frequencies as high as 100-1000 cps have been attained with quarter square multipliers. A peak multiplier

---

[*] Superscripts refer to numbered items in Bibliography.

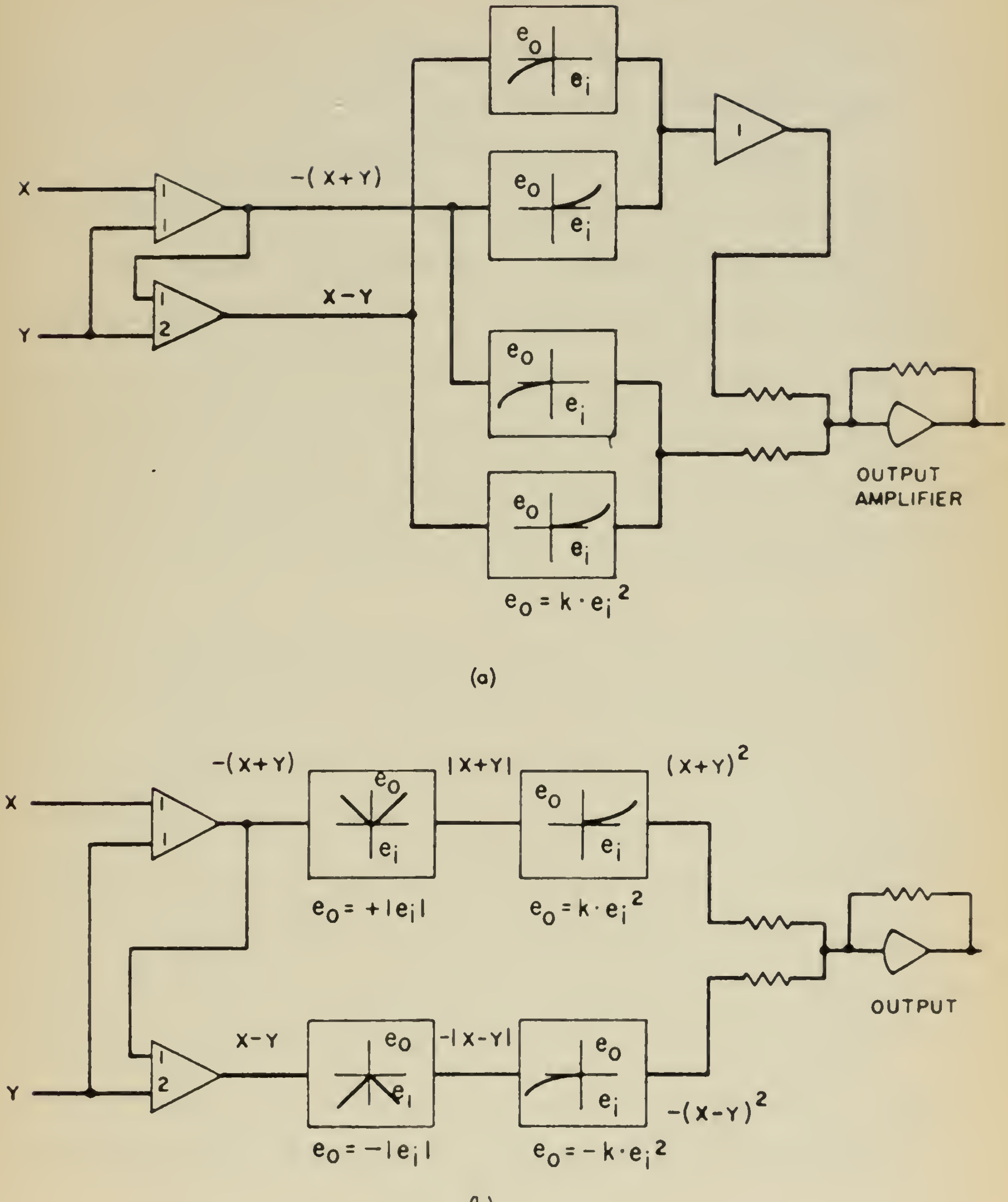

(a)

(b)

Fig. 1-3; Quarter Square Multipliers

error of 1.5 per cent was achieved by Solbakken with a very simple passive diode-resistive network.[2]

In the hybrid digital-analog scheme for aircraft flight simulation, several analog multipliers which are able to perform four-quadrant multiplication with an accuracy better than 1 per cent of full scale are needed. The required bandwidth is rather low, however, since the highest input frequencies are less than 2 cps. The analog multiplier discussed in this thesis was designed and built primarily for use in such an aircraft simulator. A prime design objective, in addition to meeting the stated accuracy and frequency requirements, was an overall reduction in the number of expensive operational amplifiers used specifically to service multipliers in the simulator. Further stipulations were that the multiplier be a solid state device with no moving parts.

The electro-optical multiplier is a direct analog to the servo-multiplier. In place of the servomechanism which positions the potentiometer shaft in accordance with the input X to the servo, this new multiplier uses an operational amplifier in a negative feedback configuration to vary the intensity of a low power lamp in accordance with the input to the amplifier. This change in light intensity causes a change in the resistance of photocells just as turning the potentiometer shaft causes a change in arm position of the pot. The circuit and detailed operation of the multiplier are discussed in Chapter II. Thus the replacement of the servo with a simple lamp driven by the output

of a solid state operational amplifier and replacement of the potentiometer with its movable shaft by several photocells connected in voltage divider circuits enabled the elimination of all moving parts. Furthermore, the required number of operational amplifiers was greatly reduced for the following reasons. The electro-optical multiplier can multiply each of several machine variables by the input to just one operational amplifier in the master loop, controlling lamp intensity. There is a buffer amplifier required to produce gain in the output stage, but this may be used for other functions. Hence it is not chargeable to multiplication. For four-quadrant operation, plus and minus each of the machine variables is required to excite the slave bridges, but the amplifiers used to generate these are not necessarily charged solely to the multiplier, since these quantities may be used elsewhere. Two quadrant operation requires only the positive quantities used to multiply the multiplicand, X. As a matter of fact, with the use of this device, the total number of amplifiers to be used in the simulator was reduced by almost one-half from the number required by a quarter-square system.

The electro-optical multiplier was accurate to within 0.62 per cent of the full scale 20 volts (± 10 volts) of the X input in laboratory tests. The frequency of the X input was limited to 4 cps because of product distortion at higher frequencies. It is believed that these results can be improved upon somewhat with further experimentation.

In Chapter II, circuit operation and some of the first experimental results are discussed, emphasizing the problems which were encountered.

The re-design of the container for the lamp and photocells is considered in Chapter III. The apparently satisfactory results obtained with the use of this new container and other circuit modifications are considered in Chapter IV for the one product, $Z = XY = X$. At this point, products accurate to better than .02 per cent of full scale had been obtained with a dynamic range of 3.5 cps. The allowable range for the input variable X was ± 2.8 volts, requiring a gain of about 3.5 on the multiplier output stage to bring the product back up to machine one. However, as discussed in Chapter V, further tests with a more compact lamp-photocell container for products other than $Z = X$, specifically $Z = \frac{3X}{4}$, $Z = \frac{X}{2}$, $Z = \frac{X}{4}$, indicated that the photocells were sensitive to the voltage impressed across them, causing unacceptable error in the zero product. In order to minimize this effect, the voltage change across the photocells had to be kept small. This in turn caused reduction of the range of X to ± 1.0 volts, requiring a gain of ten for the output stage of the multiplier. Conclusions and suggestions for some further research are included in Chapter VI.

CHAPTER II

THE INITIAL PROTOTYPE

A. Basic Circuit Components

Before presenting the basic multiplier circuit and a brief explanation of its operation, it would be well to describe the two most important components to be used. The first is an all-silicon solid-state operational amplifier produced by NEXUS Research Laboratory. The drift-stability of this device is quite comparable to competitive chopper stabilized types, it allows the use of differential inputs, and its small size and grid spaced pins enable the reduction of the dimensions of the entire multiplier package. Figure 2-1 gives the electrical characteristics at 25°C of the NEXUS DA-1 amplifier.[3] The reader may be less familiar with the second component in that it is a relatively new product by Raytheon. The Raysistor is a "four terminal electro-optical device consisting of a light source and a photocell assembled in a monel casing." Variation of the input to the light source causes a change in the photocell resistance, but no electrical connection exists between the lamp and photocell. Raysistor type CK 1102, chosen for its favorable low current, low voltage requirements, is illustrated in Fig. 2-2 along with its electrical characteristics. Figure 2-3 shows the variation in photocell resistance plotted against the control voltage to the lamp.[4]

B. Circuit Configuration

Other than the above mentioned components the circuit contains a

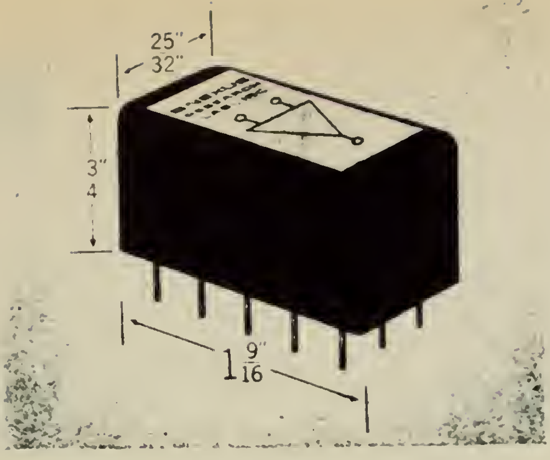

(a) NEXUS OPERATIONAL AMPLIFIER

TYPE		DA-1	BA-50	UNITS
Supply Voltage (1)		±15	±15	Volts D.C.
Supply Current		± 6	±10 N.L. ±60 max	mA D.C.
Output Voltage Range R_L 10 K	Min.	±11	$\pm 10.3^{(3)}$	Volts
Output Current Range ±10 v output	Min.	± 3	±50	mA
Common Mode Input Voltage Range	Max.	±11	—	Volts
Current Offset (Input Error Current)	Typical Max.	±30* ±90	Current Booster Amplifier for post-amplification with other amplifiers.	Nanoamps D.C.
Thermal Drift Coef. (Current Offset)	Typical Max.	—* 3.0		Nanoamps per °C
Thermal Drift Coef. (Voltage Offset)	Typical Max.	12 30		Microvolts per °C
Open-Loop Gain DC, R_L 10 K	Typical Min.	20,000 12,000		— —
DC Input Impedance	Typical Min.	200 K 100 K		Ohms
Unity - Gain Crossover Frequency	Typical	1.5		Mc Sec.
Ext Voltage Offset Trim Potentiometer (not supplied)		50 K		

(b) ELECTRICAL CHARACTERISTICS AT 25°C

Figure 2-1

(A) A RAYSISTOR

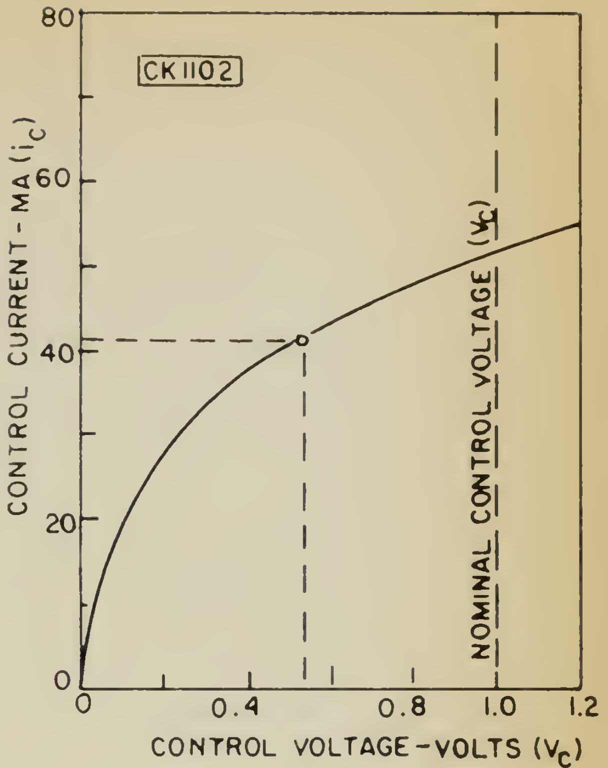

(C) i_c - V_c CHARACTERISTICS FOR CK1102

(B) CIRCUIT SYMBOL

		UNITS	CK1102
CONTROL	NOMINAL CONTROL VOLTAGE (NOTE 1)	Volts	1.0
	CONTROL VOLTAGE RANGE	Volts	0 – 1.2
	CONTROL CURRENT RANGE (CHART * 2)	mA	0 – 55
	NOMINAL CONTROL RESISTANCE	Ohms	20
SIGNAL	NOMINAL "ON" RESISTANCE (NOTE 2)	Ohms	550
	MAXIMUM "ON" RESISTANCE UNDER NOMINAL CONDITIONS (NOTE 2)	Ohms	700
	NOMINAL "OFF" RESISTANCE (NOTES 3, 4, 5)	Ohms	10^7
	MINIMUM "OFF" RESISTANCE	Ohms	10^6
	MAXIMUM SIGNAL VOLTAGE	Volts	60
	MAXIMUM POWER DISSIPATION	mW	50
	SHUNT CAPACITY	pf	4
	"SWITCH-ON" TIME (1) (NOTES 6, 8)	mSec	20
	"SWITCH-ON" TIME (2) (NOTES 6, 8)	mSec	50
	"SWITCH-OFF" TIME (1) (NOTES 7, 8)	mSec	300
	"SWITCH-OFF" TIME (2) (NOTES 7, 8)	mSec	45
	COUPLING CAPACITY (NOTE 10)	pf	0.003

(D) ELECTRICAL CHARACTERISTICS

Fig. 2-2

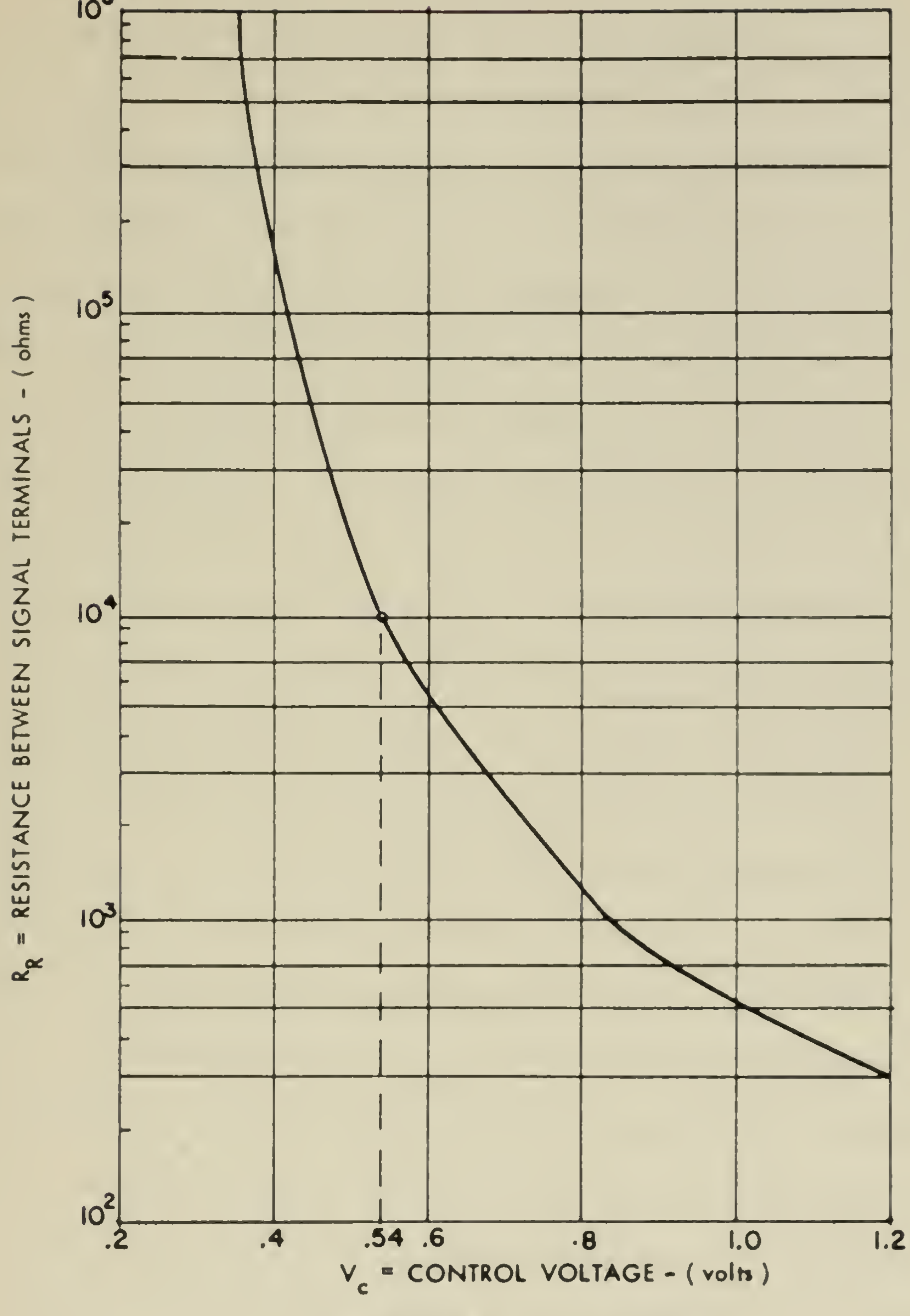

Fig. 2-3: R_R vs V_c for CK1102

NEXUS solid state booster amplifier, BA-50 whose characteristics are also shown in Fig. 2-1, and a number of precision potentiometers and resistors. The simplicity of the design is evident from the circuit diagram shown in Fig. 2-4. For purposes of simplification, we shall take the case of the product, Z, of two quantities X and Y. Suppose that X is the input to the positive terminal of the DA-1. Then the high gain of the amplifier used in the negative feedback loop forces the summing node or negative input of the amplifier to be also equal to X. This is accomplished in the following manner: Any difference in the two inputs to DA-1 is greatly amplified, causing V_c, the control voltage to the Raysistor lamp, to change in such a manner as to force R_{R3}, the photocell resistance connected in the voltage divider circuit, to take on the value required such that $V_M = X$. The 10 volt source connected in series with R_6 and the precision 100 ohm pot provides most of the current required by the lamp. The setting of the pot is determined by the amount of current drawn by the lamp in order to approximately balance the voltage divider with the loop opened at M-T and P-K, i.e. $i_c' = 0$. In the case where $R_2 = 20K$ and $R_1 = 30K$, R_{R3} must be 10 K in order that $V_M = 0$. From Figs. 2-2(c) and 2-3, we find that $V_c = .54$ volts and $i_c = i_{co} = 42$ ma. Now with the loop closed, the amplifier need only provide small plus and minus increments of current, i_c', to change R_{R3}. We see from Figs. 2-2(c) and 2-3 that as X becomes more positive R_{R3} must decrease, meaning that i_c' must be positive. On the other hand, if X is negative R_{R3} must

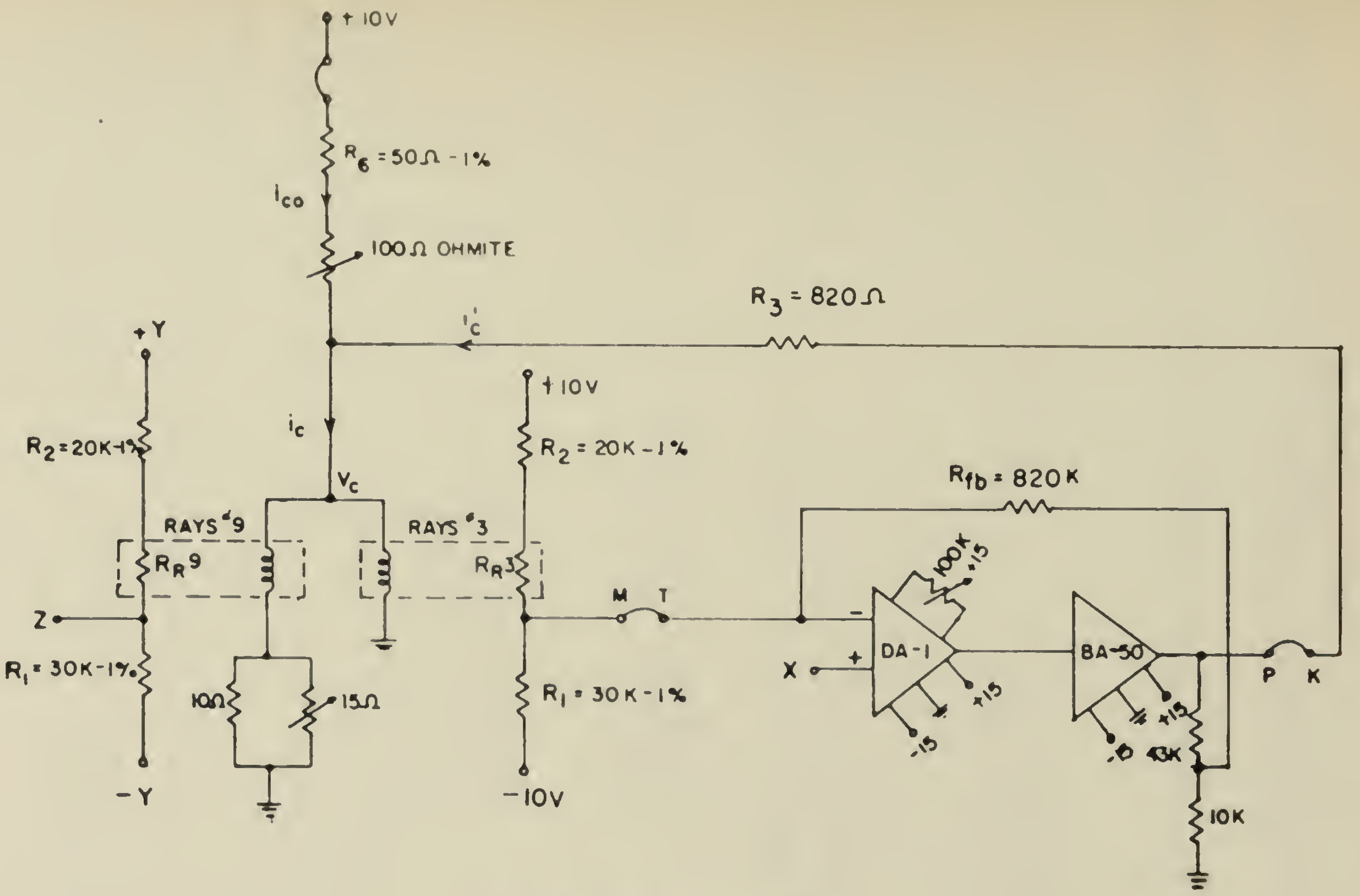

Fig. 2-4: CIRCUIT DIAGRAM
THE INITIAL PROTOTYPE

be greater than 20 K and i_c' is negative. Let us designate the voltage divider containing R_{R3} as the "master" and write the equation for V_M. Very simply,

$$V_M = X = 10 - 20 \left(\frac{R_{R3} + R_2}{R_{R3} + R_2 + R_1}\right) = 10 \left[\frac{R_1 - (R_{R3} + R_2)}{R_{R3} + R_2 + R_1}\right] \qquad (1)$$

For Z, the output of the second or "slave" voltage divider network we have

$$Z = Y - 2Y \left(\frac{R_{R9} + R_2}{R_{R9} + R_2 + R_1}\right) = Y \left[\frac{R_1 - (R_{R9} + R_2)}{R_{R9} + R_2 + R_1}\right] \qquad (2)$$

Since the photocell resistance is some function of the control voltage, let $R_{R3} = f_1(V_c)$ and $R_{R9} = f_2(V_c)$. Making these substitutions in Eq. 1 and Eq. 2, and taking the ratio of Z to X, we find,

$$\frac{Z}{X} = \frac{Y}{10} \left[\frac{(R_1 - (f_2 + R_2))\ \ (f_1 + R_1 + R_2)}{(f_2 + R_1 + R_2)\ \ (R_1 - (f_1 + R_2))}\right]$$

or

$$Z = \frac{XY}{10} \left[\frac{(R_1 - R_2 - f_2)(R_1 + R_2 + f_1)}{(R_1 + R_2 + f_2)(R_1 - R_2 - f_1)}\right] \qquad (3)$$

Thus, if we were able to obtain two Raysistors which matched perfectly, that is if $f_1(V_c) = f_2(V_c)$, then $Z = \frac{XY}{10}$ where 10 is machine 1 and we have the required product. More products such as XW , XV , XU , etc. could be obtained by connecting the lamps of more Raysistors in parallel with the master lamp, their photocells being connected in similar "slave" networks with ± W , ± V , ± U , etc. across the voltage

dividers respectively. The desired products are then taken off at the divider midpoints as in the case of Z. Suppose that the two Raysistors match perfectly at one point, where X is zero and $R_R = R_o$ for $V_c = V_{co}$. Assuming that $f_1(V_c)$ and $f_2(V_c)$ are linear over some limited range of R_R, we can write,

$$\begin{aligned} V_c &= V_{co} + \Delta V_c \\ R_{R3} &= R_o + a\,\Delta V_c \\ R_{R9} &= R_o + b\,\Delta V_c \end{aligned} \tag{4}$$

where a and b are the slightly different slopes of the two straight line approximations. Making these substitutions into Eq. 3 we find

$$Z = \frac{XY}{10} \; \frac{(R_1 - R_2 - R_0 - b\Delta V_c)\,(R_1 + R_2 + R_0 + a\,\Delta V_c)}{(R_1 + R_2 + R_0 + b\,\Delta V_c)(R_1 - R_2 - R_0 - a\,\Delta V_c)} \quad .$$

Since $R_1 = R_2 + R_0$ by definition of R_0, the above equation simplifies to

$$Z = \frac{XY}{10}\left(\frac{b}{a}\right)\left(\frac{2R_0 + a\,\Delta V_c}{2R_0 + b\,\Delta V_c}\right) = P_L \tag{5}$$

Ideally the product would be $P_T = \frac{XY}{10}$ so we find the error involved by taking

$$\Delta P = P_T - P_L = \frac{XY}{10}\left[1 - \left(\frac{b}{a}\right)\left(\frac{2R_0 + a\,\Delta V_c}{2R_0 + b\,\Delta V_c}\right)\right] \tag{6}$$

$$= \frac{XY}{10}\left[\frac{2a\,R_0 - 2b\,R_0}{2a\,R_0 + a\,b\,\Delta V_c}\right]$$

If the slopes differ by some small amount ϵ so that $b = a + \epsilon$ with $a\,\Delta V_c = \Delta R$, Eq. 6 becomes

$$\Delta P = \frac{XY}{10}\left[\frac{-2\frac{\epsilon}{a}}{2+\frac{(a+\epsilon)}{a}\frac{\Delta R}{R_0}}\right]$$

Performing the division, this becomes

$$\Delta P = \frac{XY}{10}\left[-\frac{\epsilon}{a} + \frac{\frac{\epsilon}{a}\frac{(a+\epsilon)}{a}\left(\frac{\Delta R}{R_0}\right)}{2+\frac{(a+\epsilon)}{a}\left(\frac{\Delta R}{R_0}\right)}\right] \qquad (7)$$

$$= \frac{XY}{10}\frac{\epsilon}{a}\left[\frac{\left(\frac{a+\epsilon}{a}\right)\left(\frac{\Delta R}{R_0}\right)}{2+\frac{(a+\epsilon)}{a}\left(\frac{\Delta R}{R_0}\right)} - 1\right]$$

Equation 7 shows that the error is dependent upon both X and Y to some extent. . By choosing a range of R_R where the slopes of the $R_R - V_c$ characteristics differ very slightly, the error and the non-linearities can be practically eliminated. Of course, this result depends upon the assumption that the characteristics are linear in the chosen range.

There are other considerations in choosing the operating range of the Raysistors. Experimental results summarized in Appendix I imply that there are hysteresis effects due to signal heating of the photocell and that the photocell resistance may also be sensitive to the voltage placed across it. The magnitude of both of these effects is also dependent upon the range of R_R in which we are operating.

C. Experimental Results

Since the author did not participate in the original experimental tests on the multiplier, discussion of the results will be somewhat limited

and will mainly serve to demonstrate to the reader that

1. the multiplier product was linear and
2. a definite stability problem, namely drift of the zero product, was encountered.

The first step in the experimental procedure was to obtain data and to plot the R_R versus V_c characteristics for the several Raysistors on hand. For example, Fig. 2-5 shows the characteristics for Raysistors no. 3 and no. 9. The operating range for the particular pair was chosen as 2 K to 20 K because the curves are generally of the same shape in the range. Furthermore, we are still in the range where V_c is quite low and it requires a lesser change in V_c for a given change in R_R. This is not the case for lower values of R_R as is obvious from the figure. In order to avoid heating effects, the power dissipation was limited to less than 2 milli-watts in the photocells by choosing $R_1 = 30$ K and $R_2 = 20$ K. This of course limited the possible values of X to about 1.55 volts in the positive direction and 1.40 volts in the negative direction in order to stay within the designated R_R range. In this instance Y was chosen to be 10 volts, or in the other words X was multiplied by 1. A fractional feedback arrangement was employed to reduce the gain of the entire closed loop in order to prevent oscillations. The parallel combination consisting of the 10 ohm resistor and the 15 ohm potentiometer was originally placed in the circuit to provide a zero adjustment. More explicitly, if X were made equal to zero, X being a source input, R_{R3} would be forced to be 10 K by the loop. However,

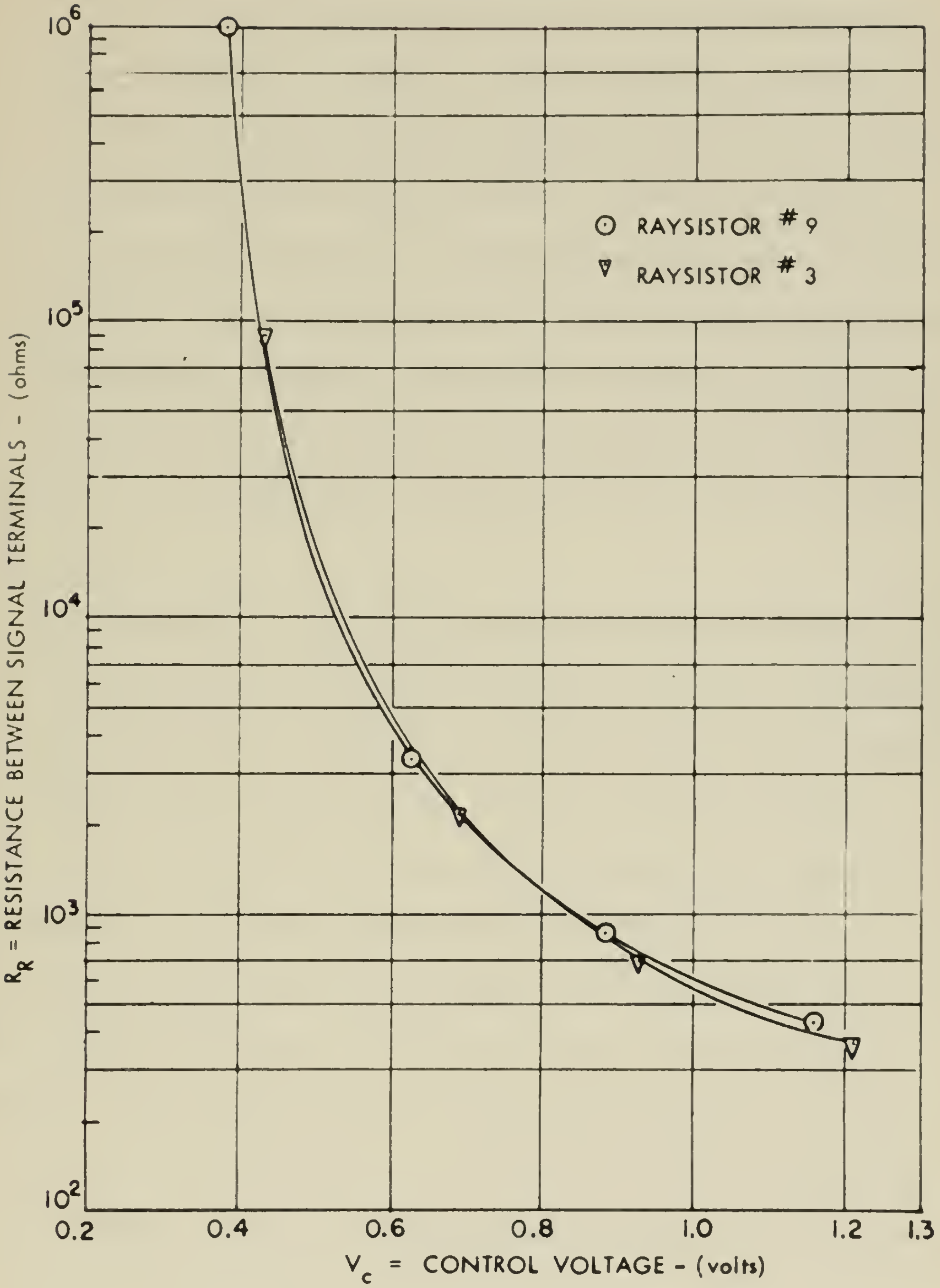

Fig. 2-5: R_R vs V_c For RAYSISTORS #3 and #9

if Raysistors no. 3 and no. 9 were slightly mismatched, the given value of V_c across the lamp of no. 9 would provide a value of R_{R9} unequal to 10 K. Thus the product, Z, would not be zero (see Eq. 2). With the trimming arrangement, the voltage across the lamp of Raysistor no. 9 was to be adjusted to give $Z = 0$ for $X = 0$. Hopefully, the pair of Raysistors would then match over the required range because of the similar general shapes of their characteristics. However, it was found that the trimming arrangement provided was very sensitive and unstable and an order had to be placed for a 10 ohm Helitrim potentiometer with infinite resolution. Since this unit was not available immediately, tests to determine linearity and drift were conducted without using the zero adjustment. This emergency procedure merely caused an offset of the entire product plot.

In Fig. 2-6 values of Z are plotted against values of the input X. The product was run out to 2 volts in both negative and positive directions in .2 volt steps, the "zero" reading being recorded three times - initially, immediately following the excursion to -2 volts, and immediately following the excursion +2 volts. The amplifier saturated, causing loop oscillations at $X = 1.743$ volts and deviation from linearity followed this. The drift of the "zero" product is evident from the three points labeled on the plot. The initial "zero" reading for Z was -.075 volts. The second "zero" reading taken after the product output excursion to -2.0 volts was -.10 volts and still drifting towards more negative values. After a 30 minute delay, waiting for the "zero"

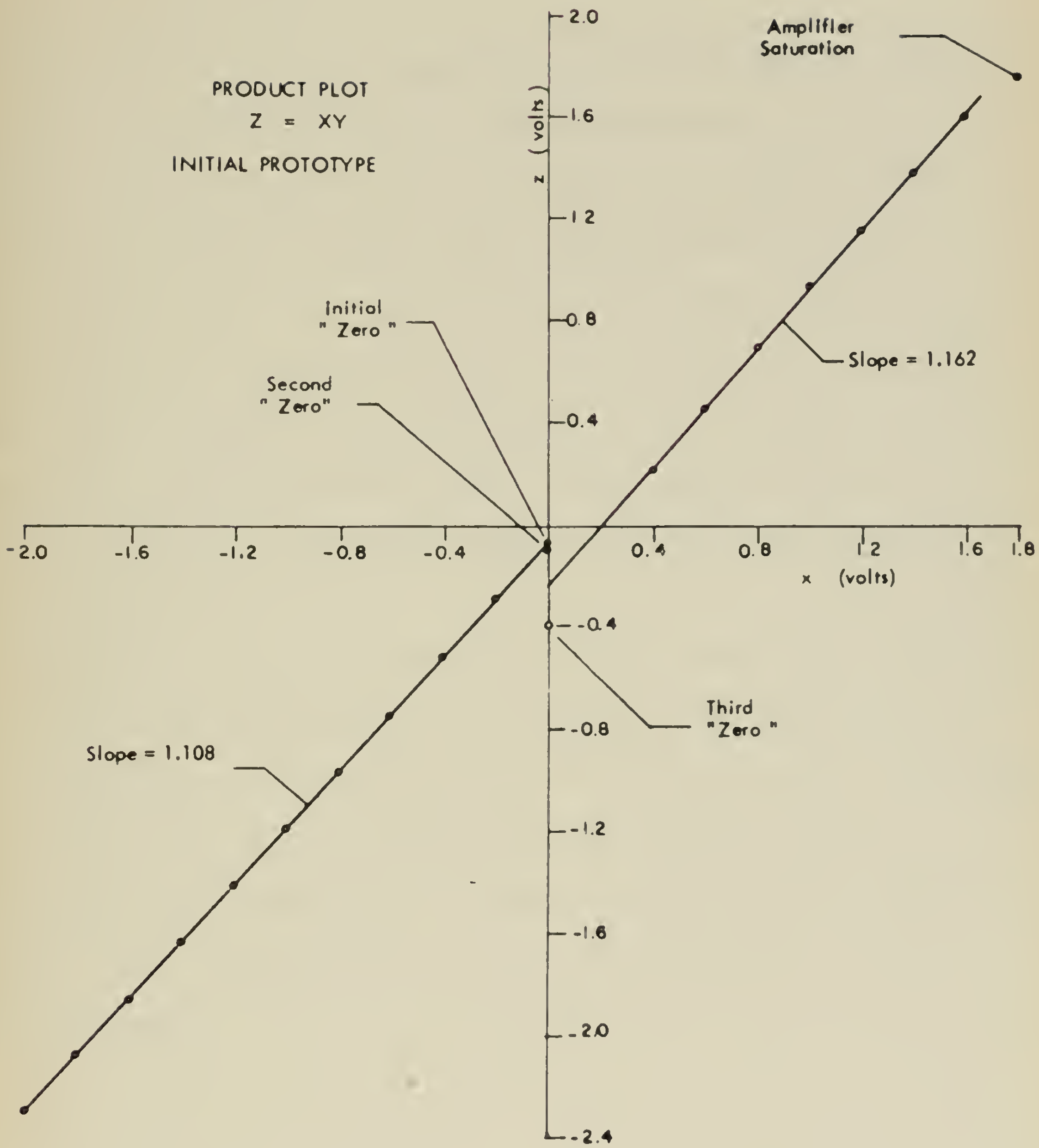
PRODUCT PLOT
Z = XY
INITIAL PROTOTYPE
Amplifier Saturation
Slope = 1.162
Slope = 1.108
Initial " Zero "
Second " Zero"
Third "Zero "
z (volts)
x (volts)
2.0
1.6
1 2
0.8
0.4
-0.4
-0.8
-1.2
-1.6
-2.0
-2.4
-2.0
-1.6
-1.2
-0.8
-0.4
0.4
0.8
1 2
1.6
1.8

Fig. 2-6

to reassume its initial value, which it did not, the positive readings were taken. By this time, the zero product had drifted to -.259 volts. Finally, a third zero reading taken after the amplifier saturated was $Z = -.40$ volts. Thus the total "zero" drift spread for the duration of the test was .325 volts.

The products in both the negative and positive regions of X are extremely linear, however. Rough calculations show that there is a maximum error of .451 per cent of full scale in the negative range and 1.78 per cent in the positive range. Although the slope of the product plots are not unity as they would be in the ideal case of multiplication of X by $Y = 1$, i.e. $Z = XY = X$, this is merely a gain factor which is easily taken care of at the multiplier output by means of an amplifier with appropriate gain. This particular amplifier need not be charged up to the multiplier proper in that it can also be used for summation of other terms.

The problem at this stage of the development was clear. First the drift of the zero product had to be eliminated. Secondly the error had to be reduced to less than one per cent of full scale value. Allowable signal levels must be high enough to require less than ten-fold amplification of the output signal, and the frequency response, also a factor, had to be flat to two or three cycles per second for use in flight simulation.

CHAPTER III

MULTIPLIER RE-DESIGN

A. Possible Causes of Instability

The prime reason for rejection of the initial prototype was the instability or drift of the zero product. Therefore, the guiding factor in designing the multiplier was the location and elimination of the source of this instability while at least maintaining the linearity of the product. It was mentioned in Chapter II with reference to Appendix I that the photocell resistance, R_R, is affected by signal heating. Since the cell in one Raysistor was completely isolated from the cell in the other Raysistor it is entirely possible that they were operating at different ambient temperatures even though the power dissipated in each was the same. It may be that one cell was able to dissipate heat more quickly than the other due to differences in photocell temperature characteristics or in the packages containing the lamp and photocell. In the Raytheon Raysistor, the lamp and the photocell are first enclosed in a common metal cylinder which is in turn encased in plastic. Experimental evidence showed that these Raysistors are extremely sensitive to environmental temperatures, even to the touch of the hand radiating body heat. There is also the possibility that history effects were causing the zero drift. If one plots the $R_R - V_C$ characteristic for a Raysistor whose photocell has not been excited by the lamp for a long period of time and the $R_R - V_c$ characteristic taken after the same photocell has been at some finite light intensity for

the same or even a shorter period, the two characteristics differ appreciably. Still another possible source of instability lies in the Raysistor lamps. They may have been heating up and cooling off at different rates and operating at different ambient temperatures thereby causing a variation in the light intensity seen by the different photocells for a given voltage, V_c. This would have caused mismatch between Raysistor pairs in addition to that caused by differences in photocell characteristics, and this mismatch might have been changing with use and aging of the lamp filament.

B. Corrective Measures

In attempting to single out any one of the above possible causes of zero drift, little success was had. Therefore, the best solution seemed to be to design a lamp-photocell package which would minimize, if not completely eliminate, all probable sources of difficulty. If all the photocells to be used were mounted on a single base, a common heat sink, this would seemingly minimize the effect of temperature differences due to lamp radiation and the environment of the cell. Furthermore, if these photocells were all illuminated by a single lamp the problem of non-uniformity amongst the various lamps for the Raysistors would be completely eliminated. Finally, with all the cells commonly illuminated by such a lamp the long term effects of hysteresis upon drift could be ruled out since all of the cells would have an identical light history, providing that the illumination of the several photoconductive cells was uniform.

With these ideas in mind, the design of the new lamp-photocell package

was accomplished in the following steps:

1. Choice of the type of photoconductive cell to be used.
2. Choice of the lamp.
3. Achievement of uniform illumination.
4. Allowance for experimental flexibility.

Each of these areas will now be discussed in more detail.

1) Choice of a Photoconductive Cell.

There were a number of factors to be considered in choosing a photocell for this application. Currently, two kinds of material, Cadmium Selenide (CdSe) and Cadmium Sulfide (CdS) are being widely used in the production of photoconductive cells. The Clairex Corporation, whose cells were used both by Raytheon and in this research, has developed five standard sensitive materials in CdS and CdSe which vary in spectral response, sensitivity, speed, temperature, and resistance characteristics. These cells can be obtained in six different types of packages of either metal or glass and of different sizes. For our application we chose CdS as the sensitive material, whereas the Raytheon Raysistor makes use of CdSe. Although CdSe has response times which are about half those of CdS and is a little more sensitive, the improved temperature characteristics and the reduced hysteresis effects in CdS outweigh these advantages. Figure 3-1 is a table showing the time constants, sensitivity peak, and temperature characteristics for both the Type 4 CdSe, which we assume Raytheon used, and the Type 5 CdS which was chosen for this research. Figure 3-2 depicts the variation of conductance with light history for these two types of photocells.[5] On the

Type 4-CdSe

Light Level-Foot Candles	.01	.1	1	10	100
Time Constant (to 1-1/e of final reading)					
Rise (seconds)	1.1	.25	.047	.010	.002
Decay (seconds)	.120	.053	.023	.010	.005
Temperature Characteristic $(100 \times \frac{Gt}{G\ 25^\circ C})$					
t					
-25°C	220	130	99	99	98
0°C	170	110	100	100	101
25°C	100	100	100	100	100
50°C	77	71	86	94	96
75°C	5	27	59	78	83

Sensitivity peak at 6900A

Type 5-CdS

Light Level-Foot Candles	.01	.1	1	10	100
Time Constant (to 1-1/e of final reading)					
Rise (seconds)	2.8	.30	.074	.021	.007
Decay (seconds)	1.3	.22	.058	.021	.014
Temperature Characteristic $(100 \times \frac{Gt}{G\ 25^\circ C})$					
t					
-25°C	115	97	93	90	94
0°C	103	97	95	94	96
25°C	100	100	100	100	100
50°C	107	109	114	115	106
75°C	114	126	131	138	105

Sensitivity peak at 5500

Figure 3-1

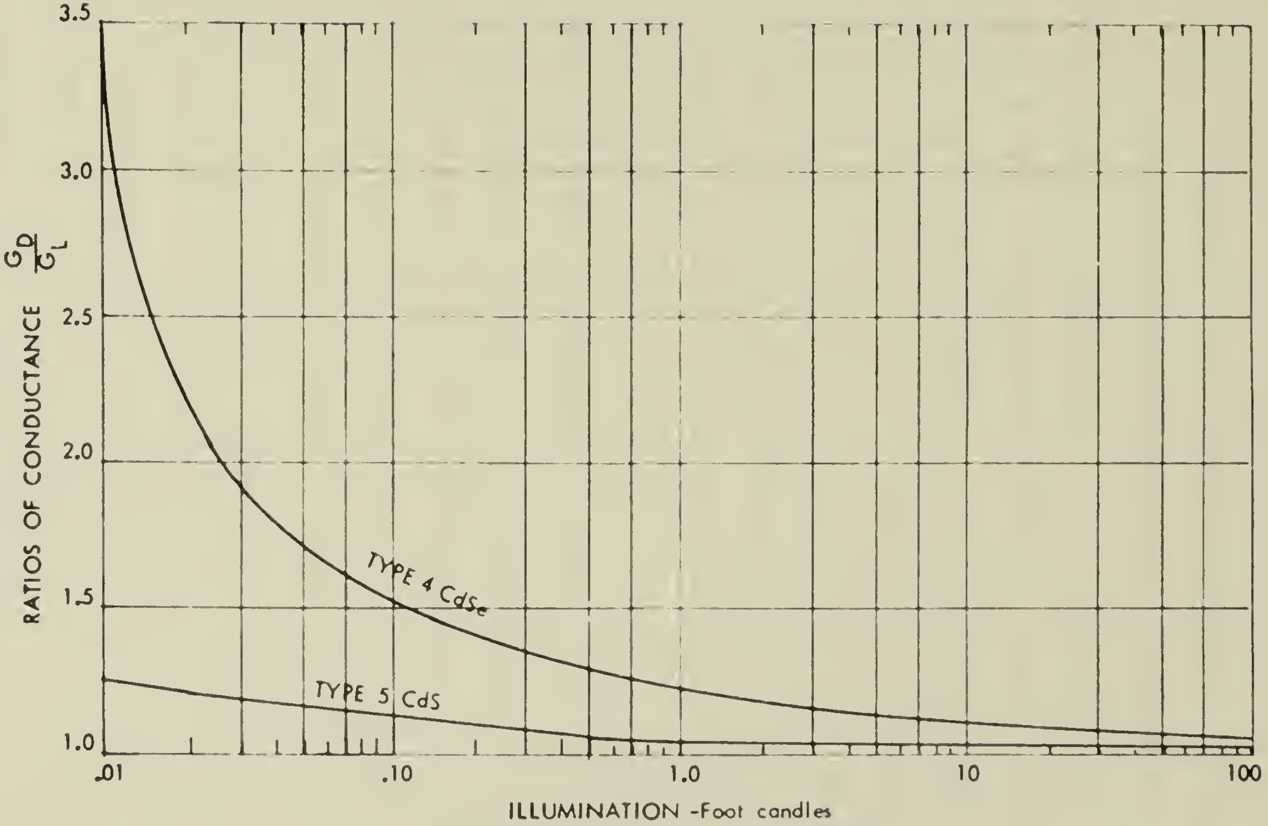

Fig. 3-2: VARIATION OF CONDUCTANCE WITH ILLUMINATION

vertical axis is the ratio of G_D to G_L where G_D is the conductivity measured from "infinite" dark history and G_L is the conductivity measured from "infinite" 30 foot-candle light history. It is obvious from this figure that CdS is somewhat less affected by history. Furthermore, in either case, it is seen to be best to operate in the range from 10 to 100 foot-candles to minimize hysteresis. If we were to operate in this range for the Type 4 CdSe the photocell resistance would run from 15 K at 10 foot candles to 7 K at 100 foot candles. For the same change in light intensity, the Type 5 CdS runs from 20 K to 93 K. Therefore for a given change in light intensity we obtain a greater variation in R_R if the CdS is used. This distinct advantage allows a wider multiplier product range without overdriving the lamp and the operational amplifier. In addition to this advantage, Fig. 3-1 shows us that if we operate in the region of 10-100 foot candles or 20 K-93 K, the rise and decay times for the CdS are comparable with those we would have obtained had we used the CdSe photocells over an increased light intensity range in order to obtain a comparable product magnitude. Actually, the speed has been found to be a square root function of light intensity.[5]

With regard to the size and type of photocell mounting which was chosen, inquiry was made into the cost and feasibility of mounting several cells on a common heat sink and hermetically sealing the entire unit. Since the expense involved in this would have been quite large with no guarantee of success, the decision was made to order a quantity of Clairex's CL605L individual photoconductive cells hermetically sealed in separate glass packages. The small size of this cell, shown

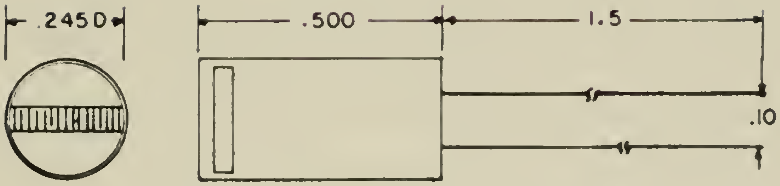

CL 605L PHOTOCONDUCTIVE CELL

Fig. 3-3

in Fig. 3-3 contributes toward compact packaging. Clairex Corporation agreed to furnish cells of this type which were individually tested and chosen for matching characteristics insofar as the state of the art would allow.

2. Choice of a Lamp

The following requirements were involved in choosing the lamp to be used as the source of photocell illumination. Power supply considerations and the desire to minimize the load on the operational amplifier posed the need for a low voltage, low current lamp. Meanwhile the lamp had to be powerful enough to enable use of the lower resistance range of R_R while still being positioned at a distance from the cells which was large enough to allow for a sufficient diffusion of the light received by the photocells. Since a low voltage, low current lamp was not immediately available, some tests were run with a Chicago Miniature no. 1768 lamp rated at 6.0 volts and .20 amps. The final and most successful experiments employed a Chicago Miniature no. 331 lamp rated at 1.35 volts and .06 amps. One evident advantage of the no. 331 lamp, besides the lower power requirements, was the improvement of the frequency response. This will be discussed along with experimental results for multiplier tests run with each of these two lamps in Chapter IV.

3. Achievement of Uniform Illumination

Having chosen the photoconductive cells and the lamp, the problem became one of arranging these components to achieve the most uniform and efficient illumination of the cells. Figures 3-4(a) - (c) include

photographs and plan drawings of the finished multiplier test rig. In order to reduce to a minimum the area requiring uniformity of illumination, the photocells were mounted on the circumference of a circle in one base of the cylinder. The lamp was mounted on the opposite base. A piece of diffusing glass was then placed between the lamp and the cells in order to scatter the light incident on the cells. This glass was spaced only one quarter of a inch from the cells, but the spacing between the lamp and glass was considered to be a bit more critical for the following reasons. In order that the light seen by the photocells be distributed uniformly over the surface of the diffusing glass, the distance between the source and the glass must be kept large in comparison with the greatest linear dimension of the source. By placing the glass at a distance which is about five times the physical length of the portion of the lamp exposed to the chamber, the best results are obtained. Finally, in order to insure even more complete diffusion of the light inside the package, the inside of the cylinder was painted with several coats of white diffusing paint, CE 350 Magnesium Carbonate distributed by General Electric. Application of the paint had to be accomplished by dipping after first cleansing the metal surfaces with a degreasant.

4. Allowance for Experimental Flexibility.

Provision for variation of the distance between the lamp and the diffusing glass was made by threading both the hollow cylinder and the base containing the lamp. This feature also allows complete

accessibility of the lamp for replacement purposes. The photoconductive cells were mounted in small shells which were also very finely threaded. These shells then screwed into the other removable base of the cylinder. Thus, with a screw driver, the distance of each photocell from the light source could be varied, compensating for any variation in light intensity on the base of the cylinder. Furthermore, this adjustment could also be used to match the "slave" cells to the "master" cell under conditions of the "master" input equal to zero, i.e. $X = 0$. These provisions for experimental flexibility resulted in the rather large overall dimensions of the lamp-photocell package.

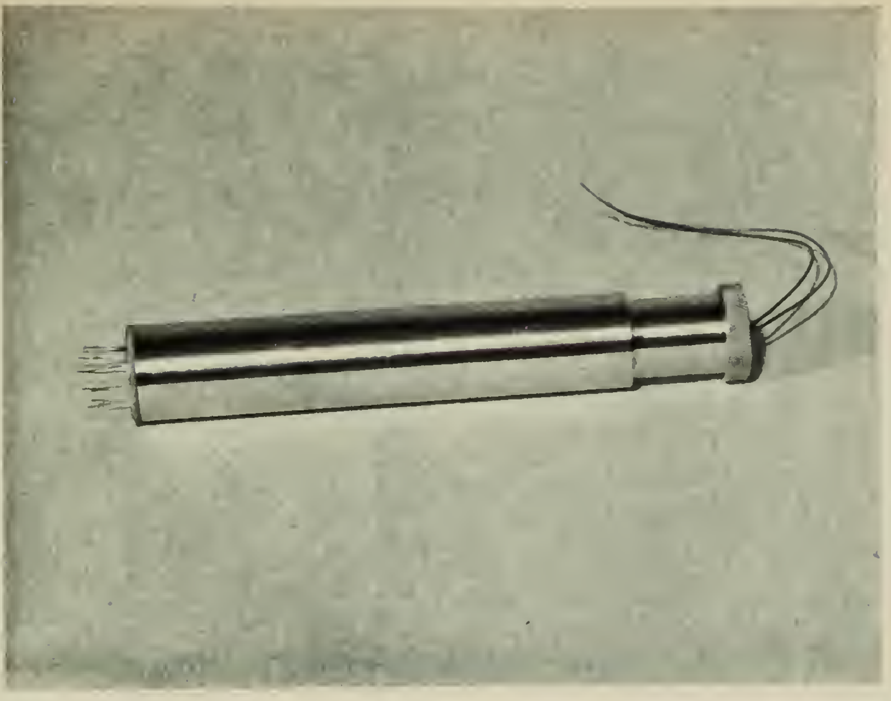

(a)

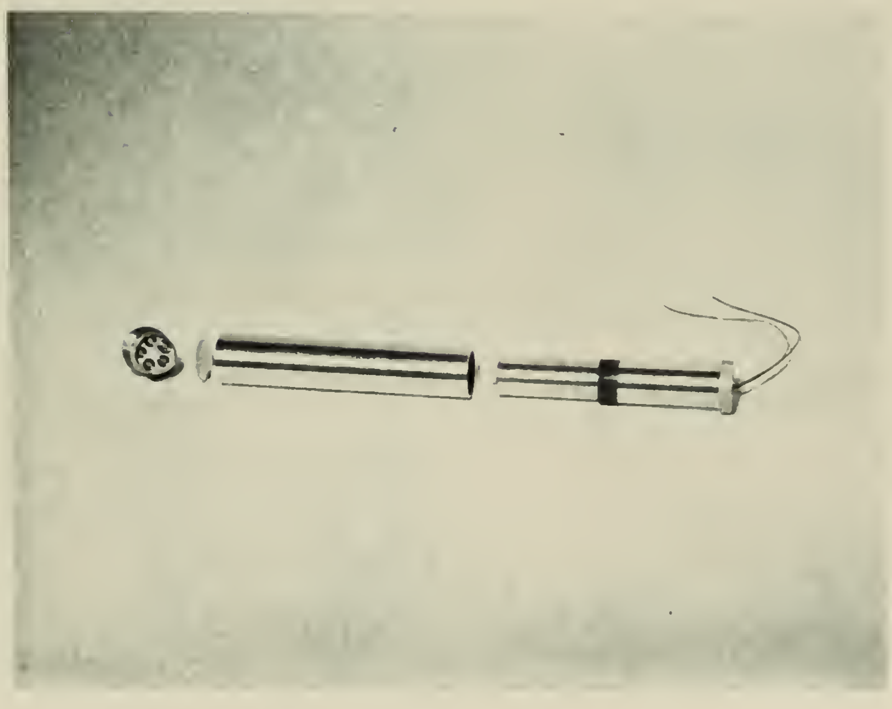

(b)

Fig. 3-4 PHOTOCELL-LAMP PACKAGE

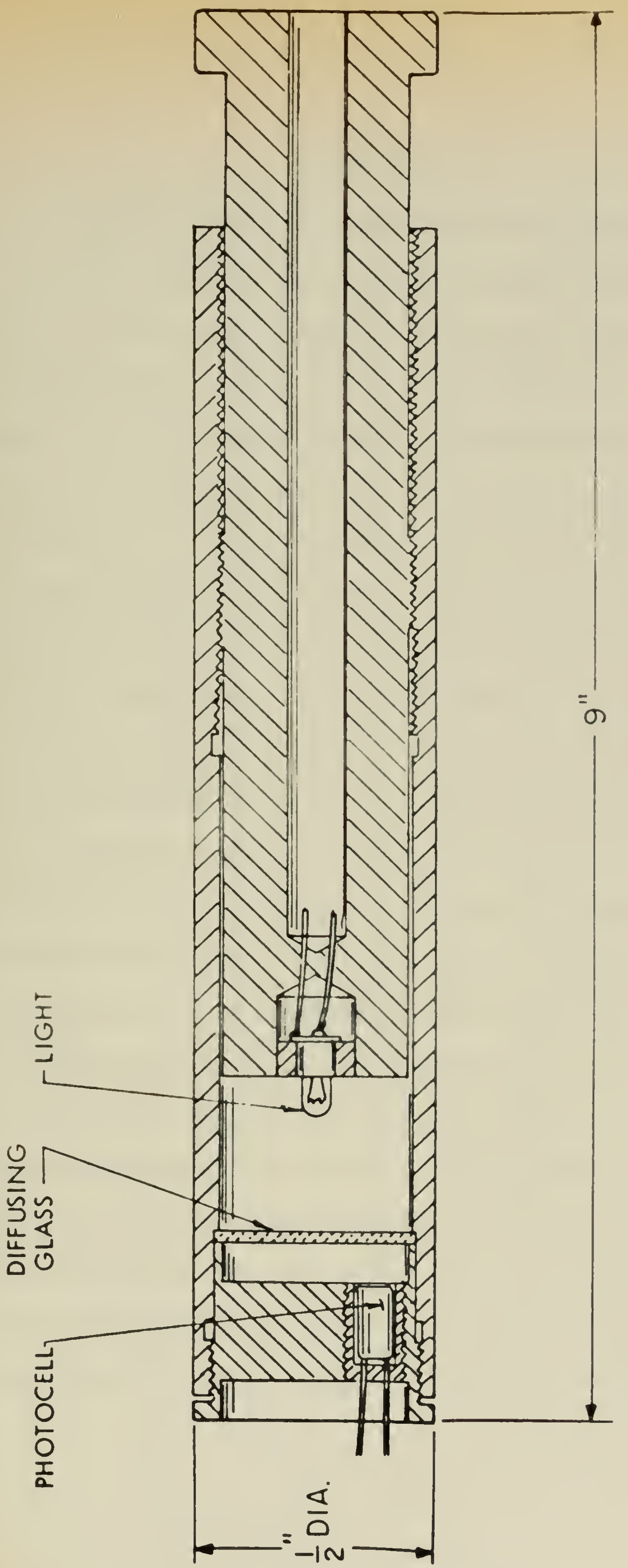

Fig. 3-4 (c): SECTIONAL VIEW OF PHOTOCELL-LAMP PACKAGE

CHAPTER IV

EXPERIMENTAL PROCEDURE AND RESULTS

At the start, the optimum range of photocell resistance to be used was an undetermined quantity. Figure 3-2 of Chapter III and the accompanying discussion led to the establishment of R_R = 100 K as a high limit for this range in order to minimize any hysteresis effects. The first step in choosing the lower limit to this range was to plot the R_R versus V_c characteristics for all of the CdS photoconductive cells on hand by placing them in the newly-designed lamp-photocell test rig in groups of five and illuminating them with the Chicago Miniature no. 1768 lamp. The experimental set-up for these measurements is shown in Fig. 4-1. The 100 K precision pot was first set at the desired value for R_R. Then the 1 K pot in the lamp circuit was adjusted to obtain an approximate null on Hewlett-Packard Model 425A null-meter. Accurate nulling was accomplished with the fine adjustment on the 100 K potentiometer, and the value of V_c was recorded. Figure 4-2 is a typical example of the results which were obtained and shows the R_R - V_c characteristics for two of the photocells. Excellent matching was evident from R_R = 10 K on up. Thus 10 K was temporarily chosen as the lower limit to usable photocell resistance.

Before proceeding with a discussion of the first significant multiplier tests, a word must be said about the problem of voltage offset trimming of the operational amplifier. The manufacturer suggests that for maximum accuracy this trimming should be done under conditions of

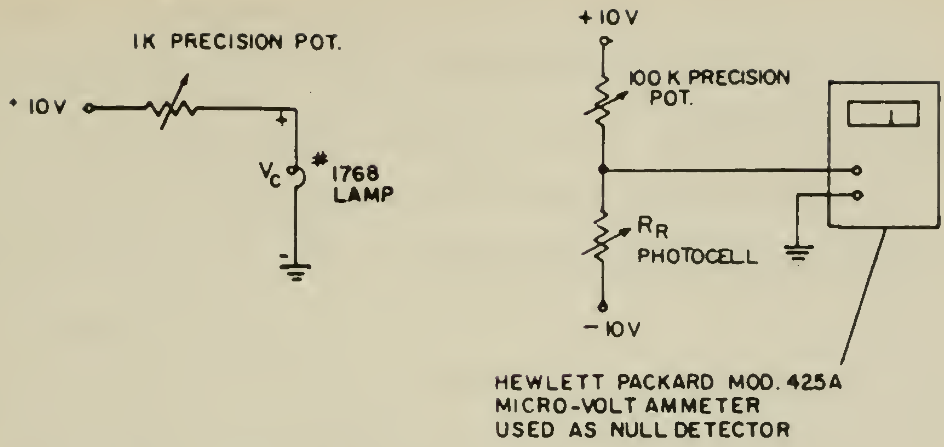

Fig. 4-1: EXPERIMENTAL SET-UP FOR DETERMINATION OF R_R - V_c CHARACTERISTICS

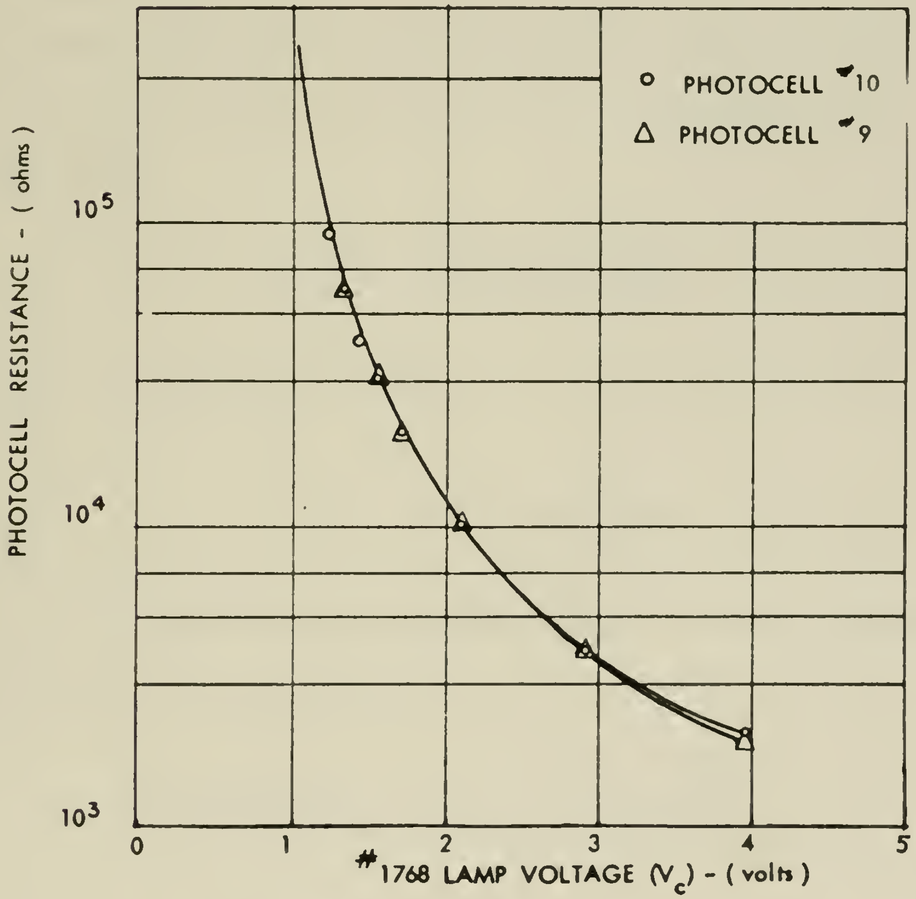

Fig. 4-2: R_R - V_c CHARACTERISTICS FOR PHOTOCELLS #9 and #10

minimum external resistance in the input terminals.[6] Figure 4-3(a) illustrates the closed-loop offset adjustment which was used. However, with the large value of R_{fb} = 820 K in the circuit of Fig. 2-4, the input current flowing through R_{fb} was causing significant voltage offset. This residual input error current was balanced out with the arrangement shown in Fig. 4-3(b) and was done after balancing for offset voltage as in (a).

Operation was confined to the 10 K to 30 K range initially. Step by step calculations and graphical constructions for setting up the multiplier circuit were as follows. Although the cells seemed to have fairly good temperature characteristics, it seemed best to limit the power dissipated in them to a reasonable extent. Thus, as a starting point, the resistor R_1 was chosen to be 30 K. From Eq. 1 of Chapter II we have

$$V_M = \frac{10(R_1 - R_2 - R_R)}{R_1 + R_2 + R_R}$$

Now if we let $\delta = R_2 + R_R - R_1$ we have

$$V_M = 10\left(\frac{-\delta}{2R_1 + \delta} \right)$$

and we can write expressions for the most positive and most negative attainable values of V_M as follows:

$$V_M \text{ (most positive)} = 10\left(\frac{-\delta_1}{2R_1 + \delta_1} \right) \qquad (1)$$

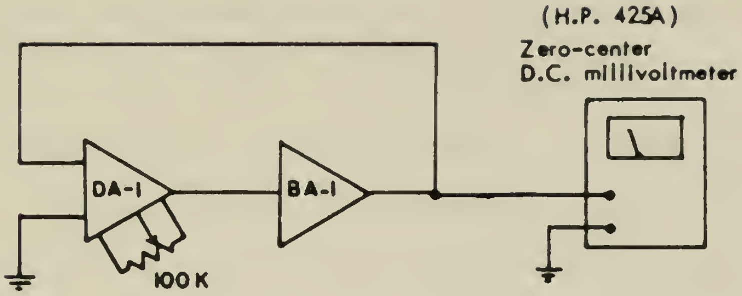

(a) OFFSET TRIMMING
THE AMPLIFIERS

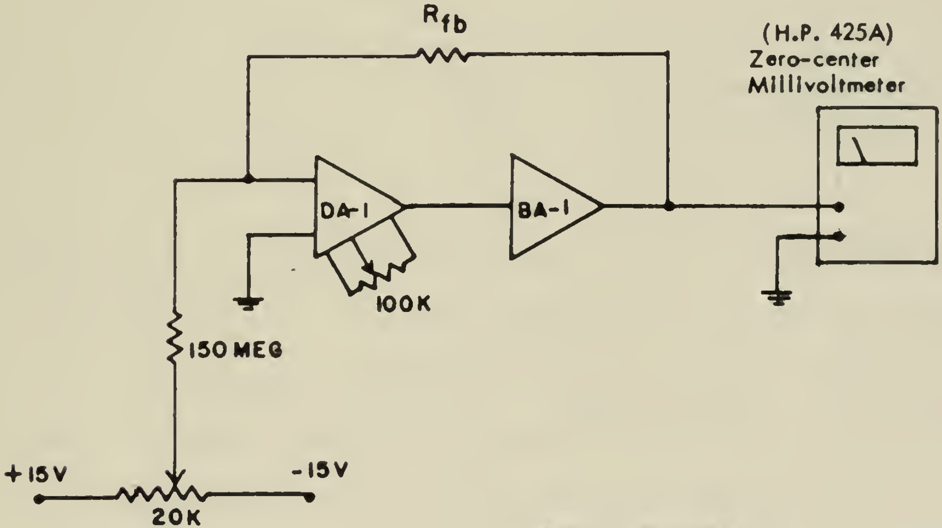

(b) CURRENT TRIMMER

Fig. 4-3

where δ_1 is negative and corresponds to the low value of photocell resistance, R_{RL}, and

$$V_M \text{ (most negative)} = 10 \left(\frac{-\delta_2}{2R_1 + \delta_2} \right) \tag{2}$$

where δ_2 is positive and corresponds to the high value of resistance, R_{RH}. Obviously then, $\delta_2 - \delta_1 = \Delta R_R$ = Photocell resistance range over which we want to operate = 20 K in this case. Letting V_M (most positive) = $-V_M$ (most negative), and substituting $\delta_2 = \delta_1 + \Delta R_R$ we obtain from Eq. 1 and Eq. 2 the following equation for δ_1

$$\delta_1^{\,2} + \delta_1 (2 R_1 + \Delta R_R) + R_1 \Delta R_R = 0 \tag{3}$$

The solution is then,

$$\delta_1 = \left(- R_1 - \frac{\Delta R_R}{2} \right) \pm \sqrt{R_1^{\,2} + \left(\frac{\Delta R_R}{2} \right)^2} \tag{4}$$

and

$$\delta_2 = \Delta R_R - R_1 - \frac{\Delta R_R}{2} \pm \sqrt{R_1^{\,2} + \left(\frac{\Delta R_R}{2} \right)^2} \tag{5}$$

In the situation under discussion with $R_1 = 30$ K and $\Delta R_R = 20$ K, we find $\delta_1 = -8.4$ and $\delta_2 = +11.6$. The value of R_2 is then easily found by $R_2 = R_1 + \delta_1 - R_{RL}$ which gives $\underline{R_2 = 11.6 \text{ K}}$. Substituting back into Eq. 1 and Eq. 2 we find V_M (most positive) = + 1.62 volts and V_M (most negative) = - 1.62 volts, thereby constraining X to this range.

The next step was to plot the load line for the circuit branch supplying

i_{co}, the major part of the current i_c required by the lamp. For the condition when $V_M = 0$ we must have $R_1 = R_2 + R_R$ or $R_R = 18.4$ K. From Fig. 4-2, we find $V_c = 1.75$ volts for this value of R_R. With the loop open and $i_c = i_{co}$, i_c must be 106 mA from the $i_c - V_c$ characteristics of the no. 1768 lamp in Fig. 4-4. The load line is then determined simply from the 10 volt source,

$$\text{Load line} = \frac{10 - 1.75}{106 \times 10^{-3}} = 78 \text{ ohms.}$$

Therefore $R_6 = 50$ ohms in series with the $100\,\Omega$ pot was sufficient to provide this resistance. The setting of the pot was made with the loop open, adjusting the pot until $V_M = 0$.

To attain the high value of $R_R = R_{RH} = 30$ K, V_c must be 1.55 volts and $i_c = 100$ mA. With the loop closed, the amplifier must then supply $i_c' = -9$ mA. For the low value of photocell resistance, $R_{RL} = 10$ K, V_c must be 2.1 volts and $i_c = 114$ mA, hence $i_c' = +13$ mA is required from the amplifier. These calculations are illustrated graphically in Fig. 4-4. In order to avoid overdriving the amplifier, $R_3 = 500$ ohms was chosen so that 15 mA could be provided at an amplifier output voltage of 7.5 volts. With these circuit parameters, power dissipation in the photocells was limited to less than 3 milliwatts.

The input variable for the D-C tests was generated by placing 10 volts across a precision potentiometer, enabling the attainment of values of X accurate to .001 volts. With the loop closed and $X = 0$, $Y = 10$ volts, a fine adjustment was made on the "slave" photocell to obtain $Z = 0$ to the nearest millivolt. Input X was then increased in

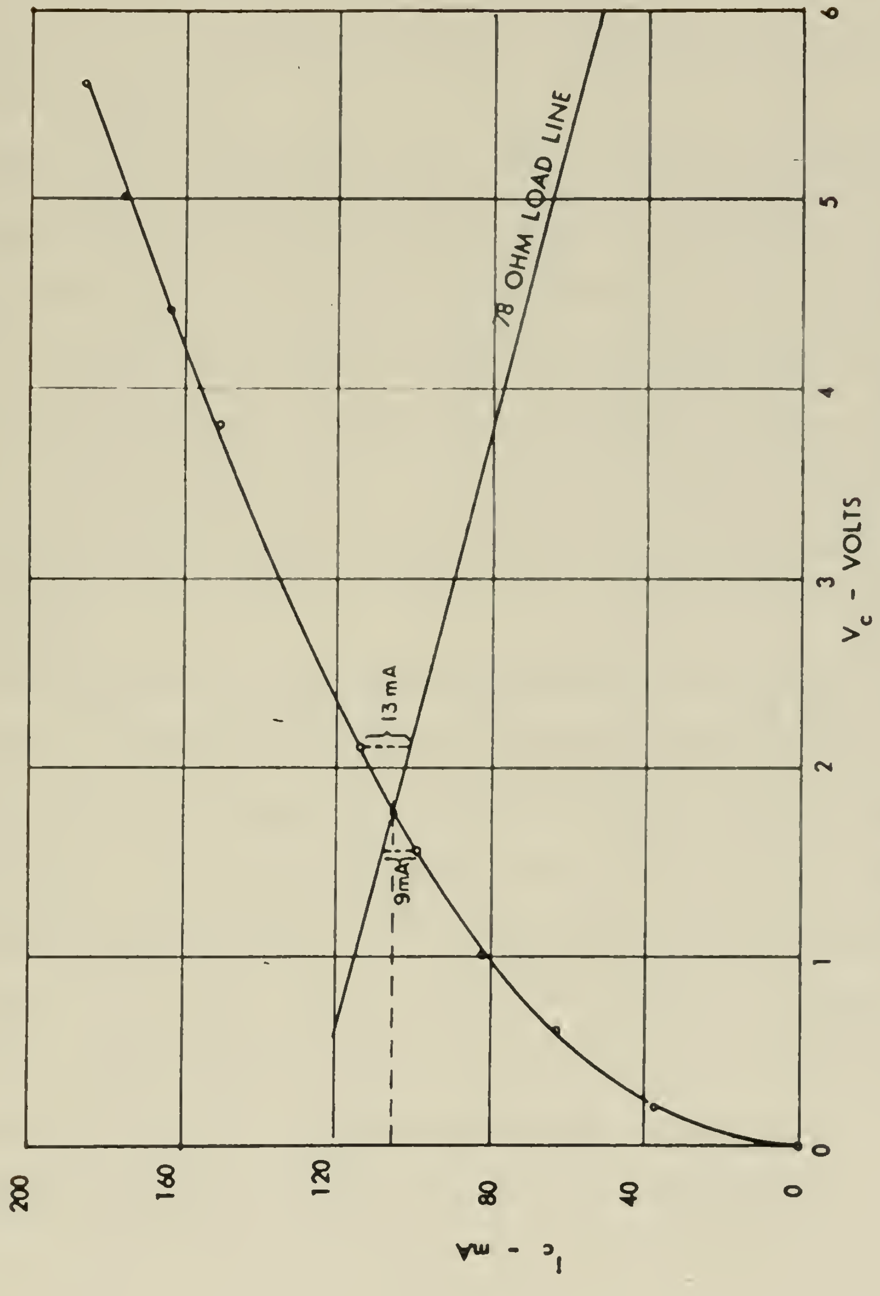

Fig. 4-4: $I_c - V_c$ CHARACTERISTIC FOR #1768 LAMP

.200 volts steps from 0.000 to 1.500 volts, and the voltages V_M and Z were recorded at each step using the same voltmeter for each reading, thereby eliminating any difference in recording instruments. From +1.500 volts, X was reduced instantaneously to 0.000 volts where checks were made for drift of the zero product. The same procedure was used in running X out to - 1.500 volts and a final check made for zero drift.

The results are plotted in Fig. 4-5. Drift of the zero product was not detectable and the product was extremely linear throughout. This preliminary check showed the error or deviation from linearity to be a maximum of 0.67 per cent of the 3.0 volt full scale product. However, results of dynamic tests were not quite so encouraging. With a 1.5 volt peak to peak sine wave input at X, the frequency range was limited to less than 1.2 cycles per second before the amplifier saturated and the product became distorted.

Reasoning that this rapid amplifier saturation with increase in frequency was in great measure due to the fact that comparatively large voltage and current changes are required at the amplifier output for a given change in R_R while operating in the low resistance range, we then experimented with even lower values of photocell resistance, the range from $R_{RL} = 3K$ to $R_{RH} = 23K$. Although this is exactly the same change in R_R, amplifier saturation occurred at less than 1.0 cps when the same 1.5 volt peak to peak sine wave was used as an input. The poor frequency response in the lower resistance

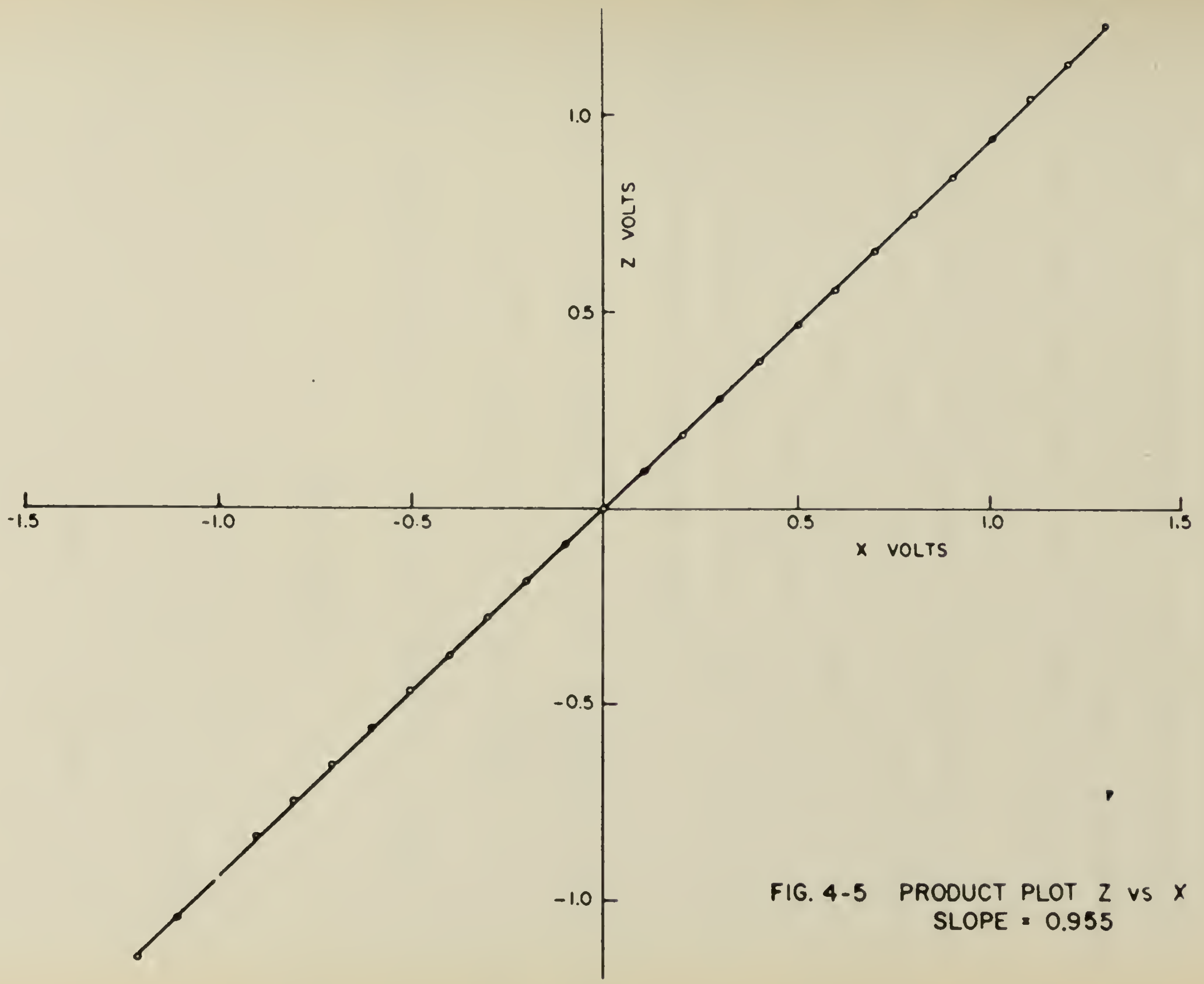

FIG. 4-5 PRODUCT PLOT Z vs X
SLOPE = 0.955

range was probably due in some part to two factors. First, as mentioned above, greater changes in control current and voltage are required. Secondly, the photocells do not matchas well on a percentage basis in the low range as they do for higher values. For example, a difference of 100 ohms between two cells operating in the 10 K range is approximately 1 per cent compared to .167 per cent in the 60 K range. The advantages seem to lie in the higher range then, providing product linearity is as good or better and zero drift is not present.

Since heating effects were not noticeable in the photocells, at least below 10 milliwatts power dissipation, resistor R_2 was eliminated from the circuitry. With this resistor removed the range of V_M and therefore of X could be extended over a greater positive and negative range for a given change in photocell resistance, $R_{RH} - R_{RL}$. Now the value of R_1 could be determined in the following manner:

$$V_M \text{ (most positive)} = 10 - 20 \left(\frac{R_{RL}}{R_1 + R_{RL}} \right) \tag{5}$$

$$V_M \text{ (most negative)} = 10 - 20 \left(\frac{R_{RH}}{R_1 + R_{RH}} \right) \tag{6}$$

and letting V_M (most positive) = $-V_M$ (most negative) we find,

$$R_1 = \sqrt{R_{RL} \; R_{RH}} \tag{7}$$

Restricting ourselves this time to $R_{RL} = 20\,\text{K}$ and $R_{RH} = 60\,\text{K}$, Eq. 7 gives $R_1 = 34.6\,\text{K}$. In this case, V_M, and therefore X, is constrained to be between ±2.5 volts. However, the required change in V_c is now only 0.35 volts in comparison to .55 volts before, while i_c'

has extreme values of - 6 mA and + 8 mA compared with - 9 mA and + 13 mA in the previous test discussed. R_3 was chosen to be 600 Ω, allowing the amplifier to provide ± 10 ma at about ± 6 volts instead of 7.5 volts which should also delay amplifier saturation.

The results of the product tests are shown in Fig. 4-6. Product error was this time roughly 0.40 per cent of the full scale 5.0 volts, and zero drift was of the order of 1 mV. The dynamic characteristics were somewhat, but not markedly, improved. Using a 2.0 volt peak to peak sinusoid input at X, the amplifier did not saturate until 1.2 cps. With the amplitude of the sine wave decreased to 1.5 volts peak to peak, the input frequency could be run out past 1.5 cps before saturation and product distortion occurred. Reducing the value of R_{fb} to 510 K did not improve the response to any noticeable extent and eliminating the β feedback arrangement did not lower the dynamic range.

These results led to the conclusion that the lamp was the prime factor in determining circuit speed. Suppose that the lamp filament can be approximated by a small body at temperature T placed in a large evacuated cavity whose interior walls are at temperature T_0. When $T - T_0$ is small, the time for the temperature of the body to change from a temperature T_1 to a temperature T_2 is given, at constant pressure, by[7]

$$\tau = \frac{C_p}{4 T_0^3 A a \sigma} \ln \frac{T_1 - T_0}{T_2 - T_0} \qquad (8)$$

where A = area of the body

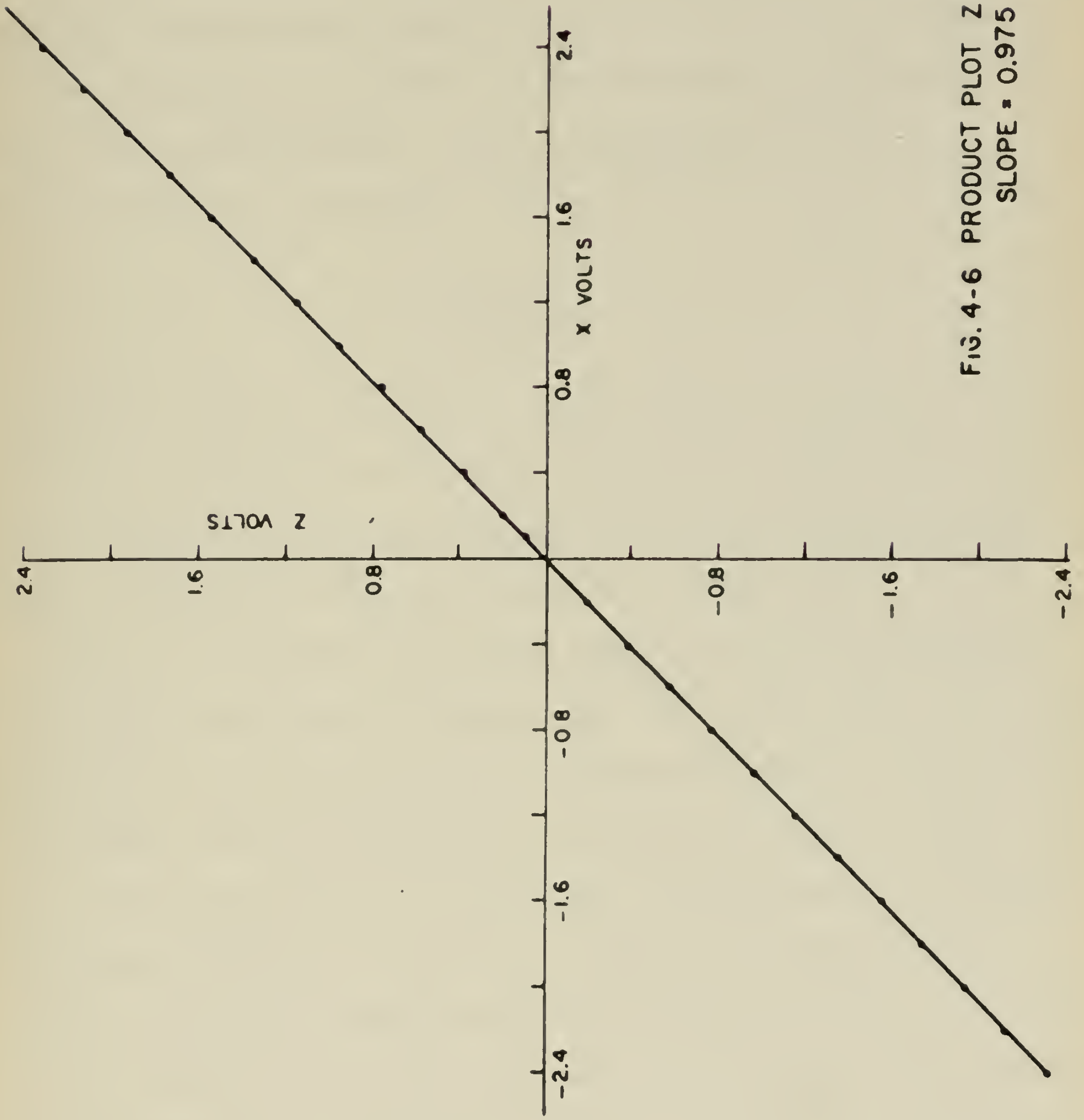

FIG. 4-6 PRODUCT PLOT Z VS. X
SLOPE = 0.975

α = absorptivity of the material

σ = Stefan-Boltzmann constant

C_p = heat capacity at constant pressure

Taking two tungsten filaments, the only variables we encounter are $C_p = mc_p$ where m is the mass and c_p is the specific heat of tungsten at constant pressure and the area, A. Therefore the time to change from one temperature to another, τ, varies as the ratio of the volume to area of the filament. Approximating the filament by a cylinder of radius r and length ℓ we have

$$\tau \propto \frac{\pi r^2 \ell}{2\pi r \ell} = \frac{r}{2} .$$

The larger the radius of the filament, the greater is τ and the slower is the response of the filament. Since a low voltage, low current lamp has a very thin wire filament, this class of lamps should enable us to increase the dynamic range of the multiplier.

With use of a lamp requiring lower voltage and current than the no. 1768, one must also expect a sizeable reduction in light output. The experiments with the no. 1768 were conducted with the lamp spaced 2 3/8 inches from the diffusing glass. With the new lamp selected, the no. 331, which is rated at 1.35 volts and 60 milliamps, the distance between lamp and glass was reduced to 1 1/4 inches maintaining the 5:1 ratio required for proper light diffusion. Once the distance parameter was fixed, new R_R - V_c characteristics had to be obtained. The minimum attainable value of R_R was 8.5K. Figure 4-7 illustrates the excellent

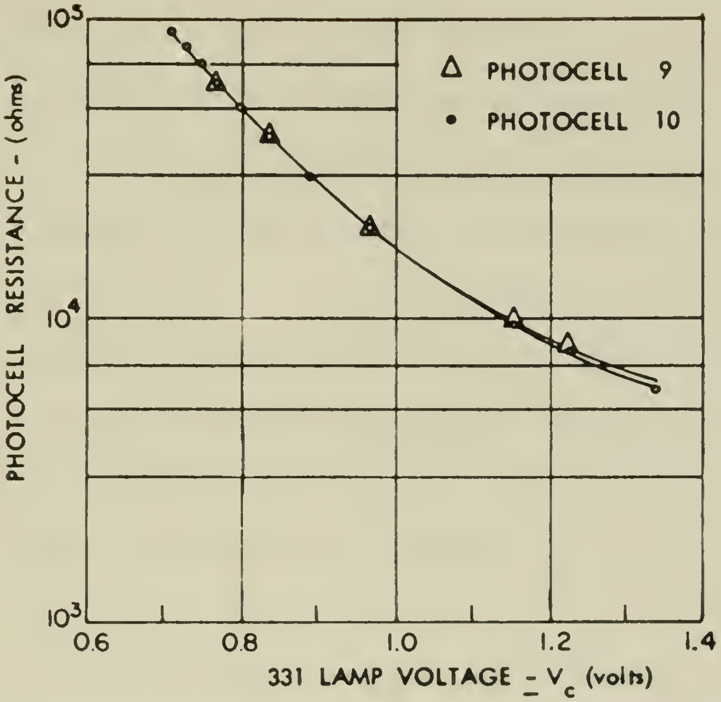

Fig. 4-7: R_R - V_c CHARACTERISTICS FOR PHOTOCELLS 9 and 10

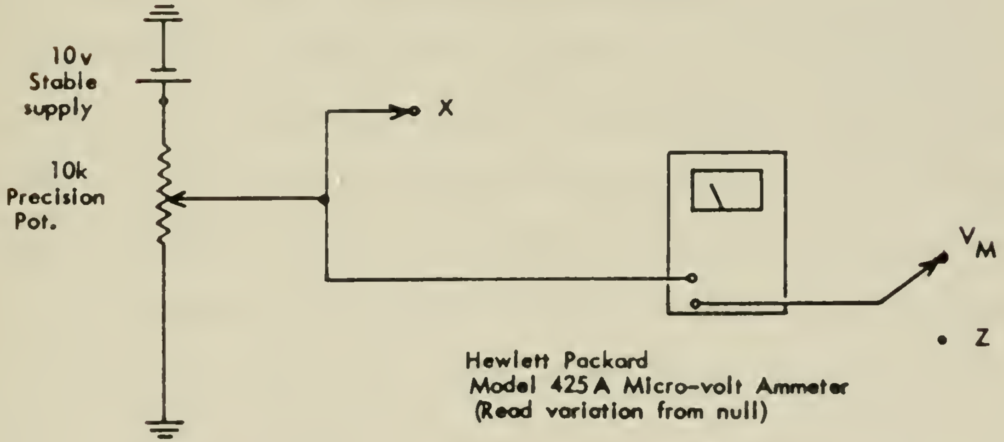

Fig. 4-8: EXPERIMENTAL SET-UP FOR ACCURATE DATA-TAKING

matching obtained over the usable range.

Utilizing the step by step set up procedure previously discussed and designing to operate between $R_{RL} = 20\text{ K}$ and $R_{RH} = 66\text{ K}$, circuit parameters were determined as follows: $R_6 = 150\,\Omega$, $R_1 = 36\text{ K}$, and $R_3 = 1\text{ K}$. The latter value was chosen so that the amplifier would be able to supply the $i_c' = \pm 3$ milliamp current required at approximately ± 3 volts. In trimming the amplifier we noted that drift of the 15 volt power sources for the current trimmer of Fig. 4-3(b) was upsetting the residual input error current balance. These sources were then replaced by very stable 10 volt power supplies. There was no change in the experimental procedure except that provision was made for more accurate recording of data. Figure 4-8 shows the set-up used. With the nullmeter connected as shown, accurate readings to the nearest millivolt were possible.

Figure 4-9(a), the product plot, and Fig. 4-9(b), a table showing the multiplier error calculations summarize the results obtained. The product is indeed linear,the maximum error being .018 per cent full scale. Furthermore, results of the dynamic tests were satisfactory. A 4.4 volt peak to peak sinusoid was used as the input at X and the frequency was varied out to 5.0 cps while making observations at V_M, the output of the BA-50 amplifier, and at Z. Figure 4-10(a) shows the amplifier output at 2.0 cps, 2.75 cps, and at 3.5 cps just before saturation. It is believed that the momentary oscillations evident in the latter two waveforms may have been caused by excurion of R_R to a very low value. That is, since

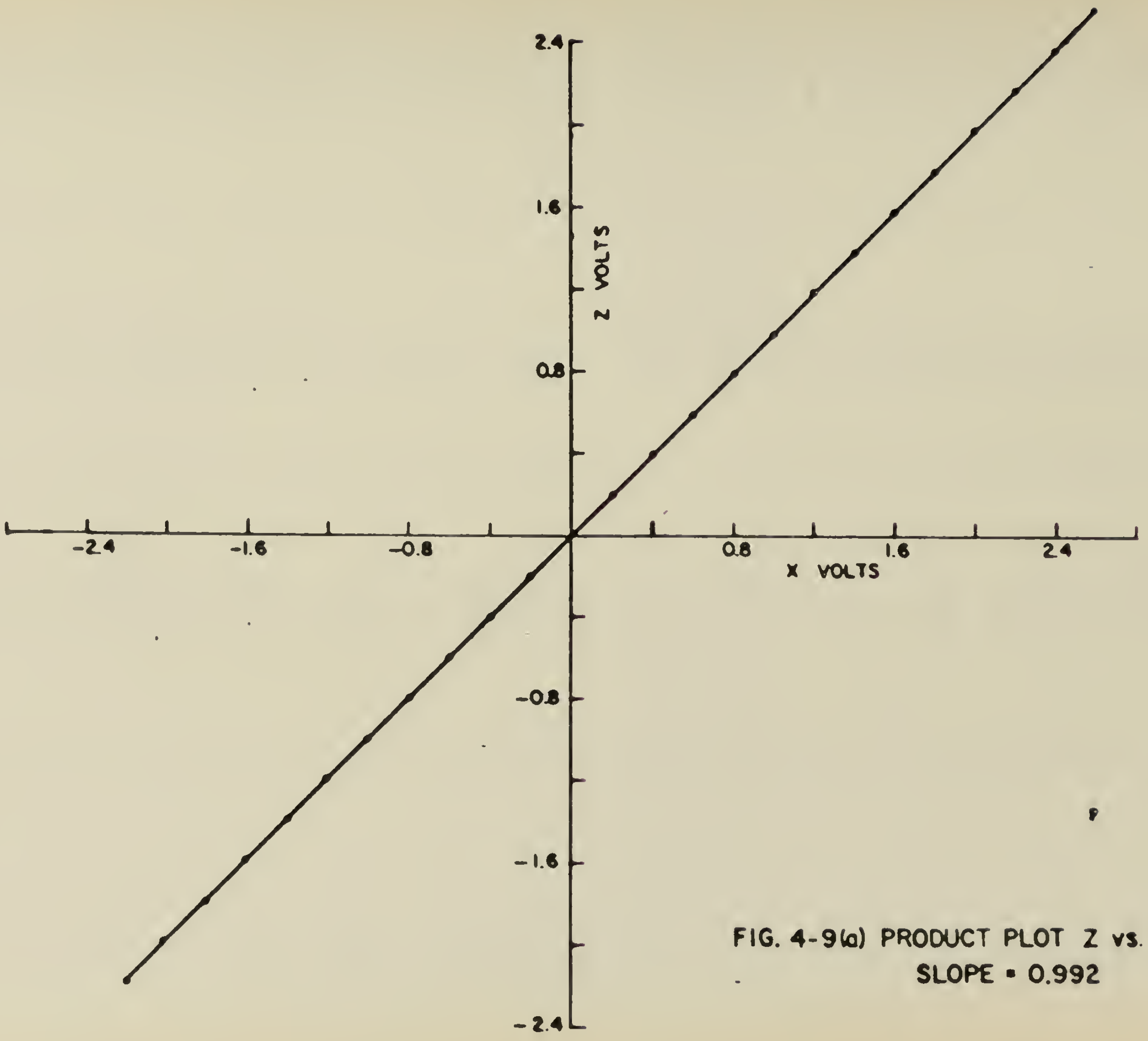

FIG. 4-9(a) PRODUCT PLOT Z vs. X
SLOPE = 0.992

Error Calculations for Multiplier

Z (Theoretical)	Z (Actual)	Error (% Full Scale)	Error (% Theoretical Value)
.198	.198	0	0
.397	.396	.018	.252
.595	.594	.018	.168
.794	.793	.018	.126
.992	.991	.018	.101
1.190	1.190	0	0
1.389	1.388	.018	.072
1.587	1.587	0	0
1.786	1.785	.018	.056
1.984	1.984	0	0
2.182	2.183	.018	.046
2.381	2.381	0	0
2.579	2.580	.018	.039
2.778	2.779	.018	.036
-.198	-.199	.018	.505
-.397	-.398	.018	.252
-.595	-.596	.018	.168
-.794	-.794	0	0
-.992	-.992	0	0
-1.190	-1.191	.018	.084
-1.389	-1.389	0	0
-1.587	-1.588	.018	.063
-1.786	-1.786	0	0
-1.984	-1.984	0	0
-2.182	-2.183	.018	.046
-2.381	-2.381	0	0
-2.579	-2.580	.018	.039
-2.778	-2.778	0	0

Figure 4-9(b)

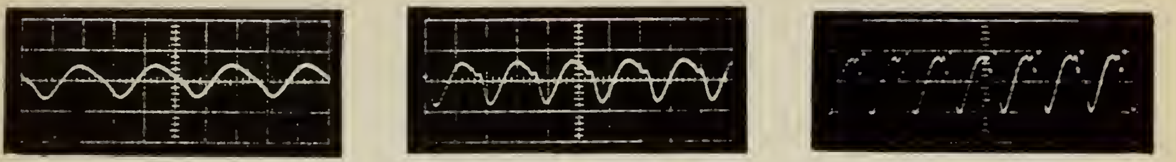

2.0 cps

2.75 cps

3.5 cps

10 volts/cm

0.2 sec/cm

(a) Amplifier Output at 2.0, 2.75, 3.5 cps

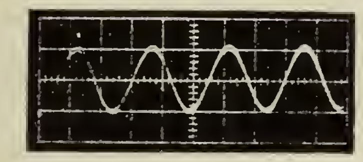

(b) X and Z at 2.0 cps

2 volts/cm

0.2 sec/cm

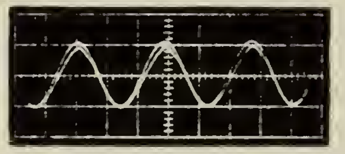

(c) X and Z at 3.5 cps

2 volts/cm

0.1 sec/cm

(d) X and Z at 4.0 cps

2 volts/cm

0.05 sec/cm

Fig. 4-10

the gain of the loop may be approximated by $\frac{R_{fb}}{R_{in}}$ where R_{in} is the parallel combination of R_1 and R_R, an unusually low value of R_R might cause the gain to rise above that value at which loop oscillations occur for a short time. Although there were no oscillations present in the D-C tests out to ±2.8 volts, further checks showed that the amplifier output voltage was peaking at a higher value, giving more light output, in the dynamic tests at frequencies higher than 2.75 cps. A superposition of the input at X and the product output at Z at 2.0 cps is shown in Fig. 4-10(b), and the same variables at 3.5 cps are shown in Fig. 4-10(c). With the exception of a slight amplitude difference as would be expected from the D-C product data, there is very little difference or distortion in the waveforms. However, after amplifier saturation, the product does begin to distort as is illustrated by Fig. 4-10(d) taken at 4.0 cps.

Having been somewhat assured by the above results that an extremely accurate linear product with little or no zero drift was attainable with a dynamic range sufficient for flight simulation, plans for the design and test of a much smaller lamp-photocell package were begun, upon which further tests could be run.

CHAPTER V

FINAL DESIGN OF THE MULTIPLIER

A. The Lamp-Photocell Package

Figure 5-1 gives a sectional view of the redesigned lamp-photocell package. Dimensional requirements were that the entire multiplier circuit, less operational amplifiers and their trimming circuitry had to fit onto a 3" x 4" card which would then be piggy-backed on a standard 4" x 8" DEC plug-in card containing the master amplifier. The height of the photocell-lamp package was to be limited to less than 1" so the flat rectangular configuration was chosen. By placing the lamp on the same side of the chamber as the photocells, reduction of the overall length dimension was achieved. The lamp, enclosed in a socket with a plastic diffusing cap, was insulated from the photocells and was recessed to prevent direct rays of light from falling on the cells. The entire chamber was again painted white and the distance of the rear reflecting wall from the cells was adjustable, allowing experimental determination of the best position. Eight photocells were mounted in order to provide for the maximum requirement of seven products. These were again inserted in adjustable shells, but a worm arrangement was used to move them back and forth instead of the previous screw adjustment. With this method the photocell leads did not twist and did not have to be disconnected and connected while making zero adjustments.

Unfortunately, this scheme was unsuccessful. Although a sufficient

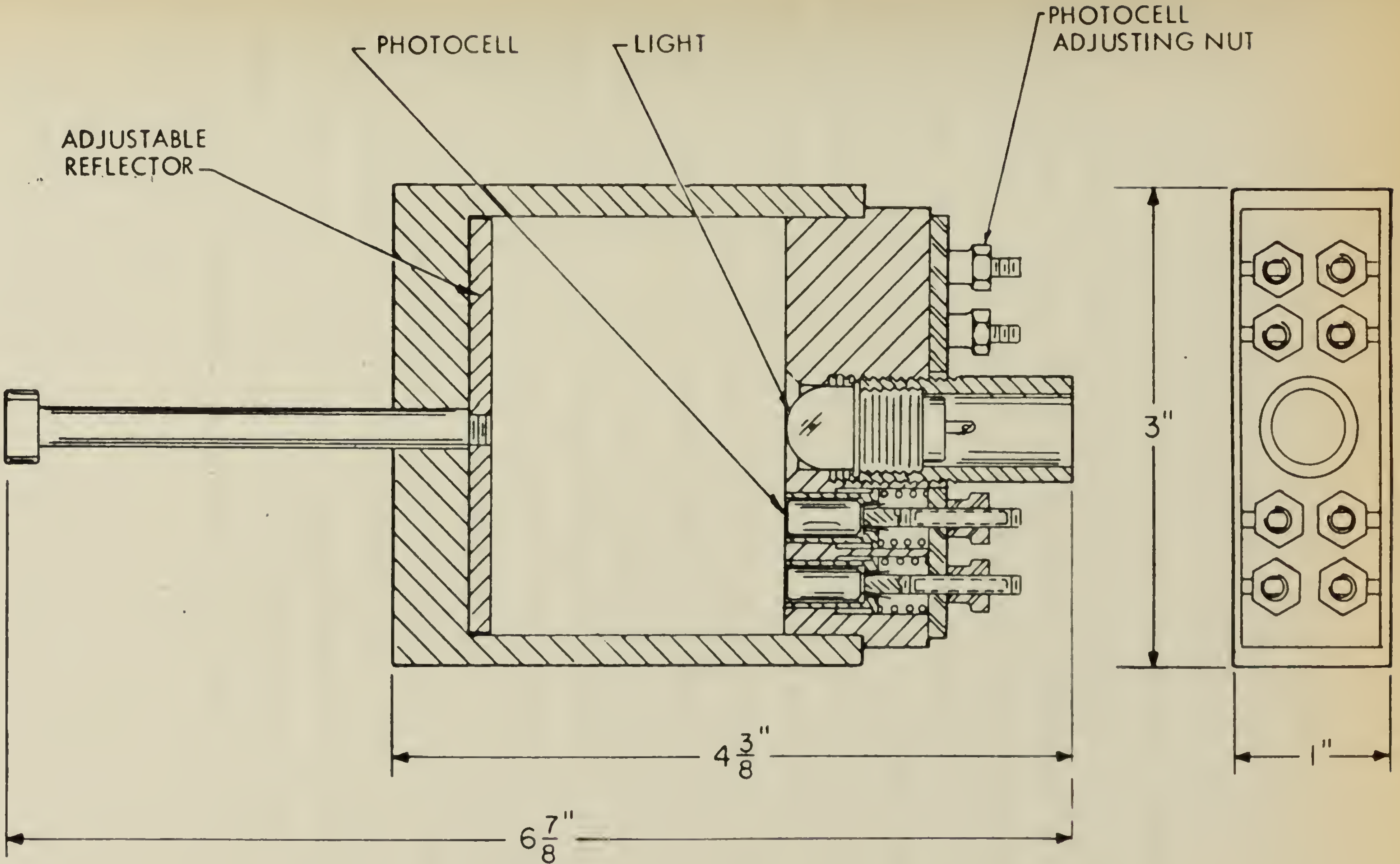

Fig. 5-1: SECTIONAL VIEW OF PHOTOCELL-LAMP PACKAGE

range of photocell resistance from 10K on up was attainable, moving the photocells towards and away from the back wall of the chamber had no noticeable effect on cell resistance. Perhaps the effective distance from the light source was too great in comparison with the allowable adjustment range. Therefore, the decision was made to move the lamp to the rear wall as in the original package. Modification was accomplished by merely removing the sliding rear wall and sinking and threading a hole for the lamp socket in the portion which had acted as a bearing for the shaft. The hole left on the photocell side was plugged, and a piece of white plastic, more opaque than the glass used in the first package, was placed between lamp and cells at a distance of 1/4" from the cells. With the arrangement three of the photocells closest to the center could be matched at zero. Varying the distance between the back wall containing the lamp and that holding the photocells did not improve upon this condition. Obviously moving all of the photocells in towards the center of the wall, filling the vacancy left by the lamp is probably the solution to the problem. However, time being an important consideration the necessary tests had to be conducted with the three usable photocells. With the back wall moved in to a point 1 1/16" from the photocells and the lamp socket adjusted so that the tip of plastic cap was 5/8" distant from the cells, good matching and a photocell resistance range of 11K on up to higher values was obtained.

B. Voltage Sensitivity

With physical parameters fixed and additional stable power supplies

now on hand, product tests were now scheduled over the whole range of the input Y. All data in the past was for $Y = 10$ volts, 1 machine unit. The chosen values of Y were $Y = 10.0$, 7.5, 5.0, and 2.5 volts giving the products $Z = X$, $\frac{3X}{4}$, $\frac{X}{2}$, and $\frac{X}{4}$ respectively. With $Y = 10.0$ volts, standard procedure, as discussed previously, was used to set $Z = 0$ with $X = 0$. The value of R_1 was still 36K in the this case. Now a preliminary check was made to determine whether changing successively to 7.5, 5.0 and 2.5 volts had any effect upon the zero product. The data presented in Fig. A-4 of Appendix I would seem to indicate that there should have been no change in the zero product. However, this data wasnot accurate enough to reveal the existence of a voltage effect on resistance in the photocells. Actually the slight deviations from linearity in the characteristics of Fig. A-4 represent deviations as much as 1K or more in photocell resistance in the 30K range. The fact that these CdS photocells are indeed sensitive to the voltage impressed across them became obvious when the value of Y was changed. As a matter of fact, when the zero product was adjusted with $Y = \pm 10$ volts across the slave voltage divider, there was a total change of .096 volts as Y was changed from 0 to 10 volts. This corresponds to an equivalent increase of about 1.3K from $R_R = 36K$. The table presented in Fig. 5-2 further confirms the voltage sensitivity of the cells. The zero product was adjusted with all possible values of Y from 1 to 10 volts across the slave divider. In each case the same results were noted. When Y was made greater than the value at which zero was set, the photocell resistance decreased. With lower values of Y, the resistance increased.

Zero set at Y =	±2	±4	±6	±8	±10
Reading at Y = ±2 (volts)	-	-0.007	-0.016	-0.027	-0.037
Equivalent change in R_R (ohms)	-	+244	+555	+932	+1271
Reading at Y = ±4 (volts)	+0.013	-	-0.018	+0.039	-0.060
Equivalent change in R_R (ohms)	-227	-	+314	+676	+1034
Reading at Y = ±6 (volts)	+0.047	+0.027	-	-0.046	-0.066
Equivalent change in R_R (ohms)	-544	-314	-	+532	+762
Reading at Y = ±8 (volts)	+0.102	+0.076	+0.042	-	-0.042
Equivalent change in R_R (ohms)	-881	-659	-366	-	+369
Reading at Y = ±10 (volts)	+0.180	+0.149	+0.105	+0.052	-
Equivalent change in R_R (ohms)	-1238	-994	-727	-362	-

Figure 5-2: Voltage Sensitivity Data

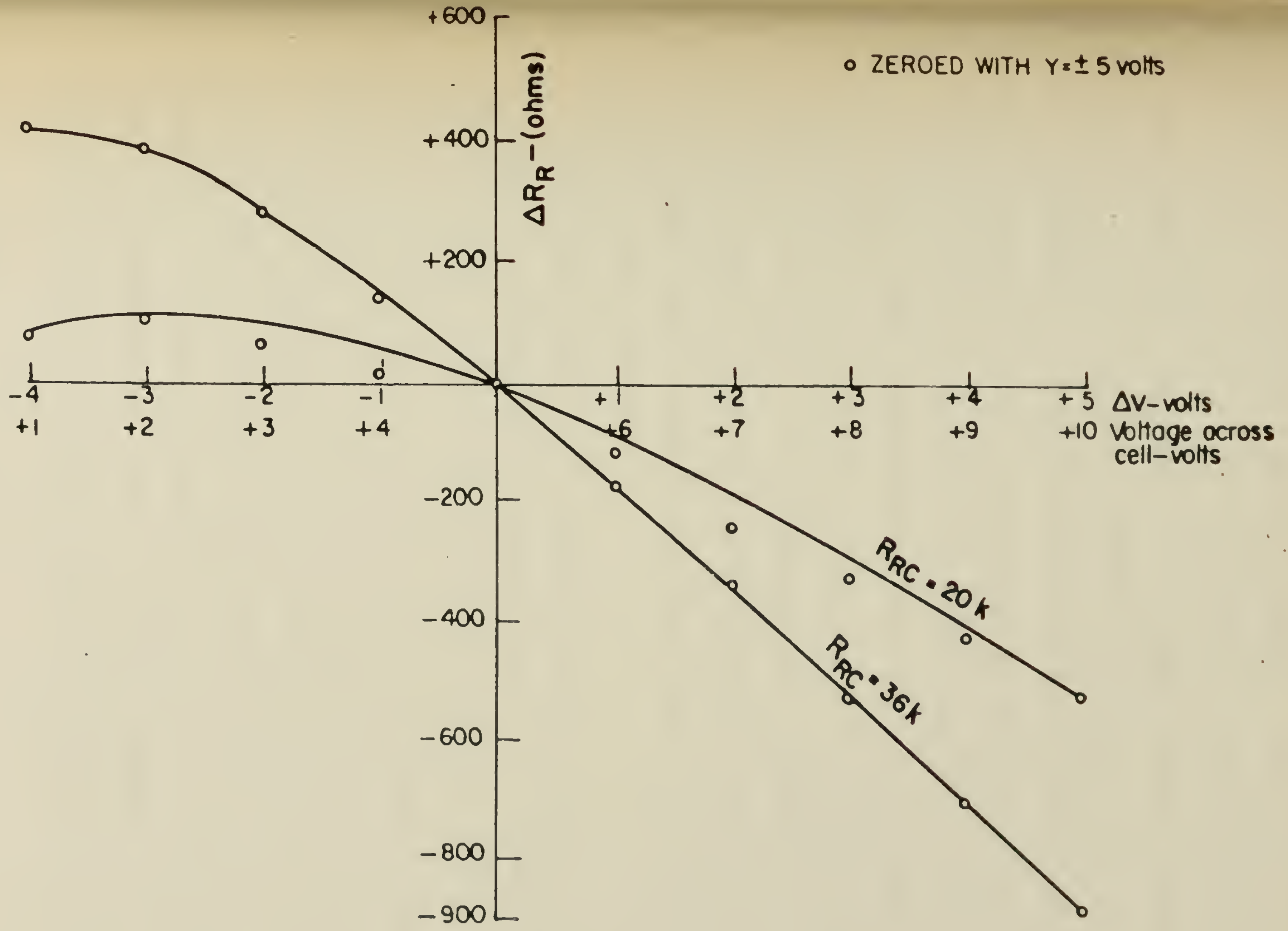

o ZEROED WITH Y = ± 5 volts
ΔR_R – (ohms)
+600
+400
+200
-200
-400
-600
-800
-900
-4
-3
-2
-1
+1
+2
+3
+4
+5
ΔV–volts
+1
+2
+3
+4
+6
+7
+8
+9
+10
Voltage across cell–volts
R_{RC} = 20 k
R_{RC} = 36 k

Fig. 5-3

This voltage sensitivity was not as pronounced when operating at lower values of R_R. That is to say if R_1, the fixed resistor in the bridge were replaced by a smaller resistance, requiring R_{RC}, the value of R_R at $Z = 0$ to be less, there was less change in the zero product and in R_R when Y was varied from 0 to 10 volts. Figure 5-3 shows ΔR_R, the variation from R_{RC} plotted versus ΔY the change in Y from the value at which the initial zero adjustment was made (5 volts in this case). The plot shows that in both cases, the voltage change across the photocell should be limited. In the instance where $R_{RC} = 20K$, a swing of 1 to 5 volts across R_R causes a ΔR_R of only about 110 ohms or 0. 55 per cent. The same change in voltage across R_R when $R_{RC} = 36K$ causes a ΔR_R of 420 ohms or 1. 16 per cent. Thus we see that it is best to operate in the lower range of R_R and to limit the change in voltage across R_R in order to minimize voltage effects.

By placing another 30K resistance in series with R_R and making $R_1 = 50K$, the voltage change produced across $R_{RC} = 20K$ in changing Y over its whole range of 0 to 10 volts was limited to 4 volts. However, this limited the input range of X to ±1. 0 volts. Therefore, a gain of 10 was required on the output stage to bring the product back up to machine 1. Figure 5-4 shows the final circuit diagram including the output amplifier stage. The 200K resistor connected between ground and the midpoint of the master voltage divider provides for equal loading of the master and slave circuits. CDA-3 is another high gain, solid state operational amplifier by Nexus. The 300 ohm resistor in series with

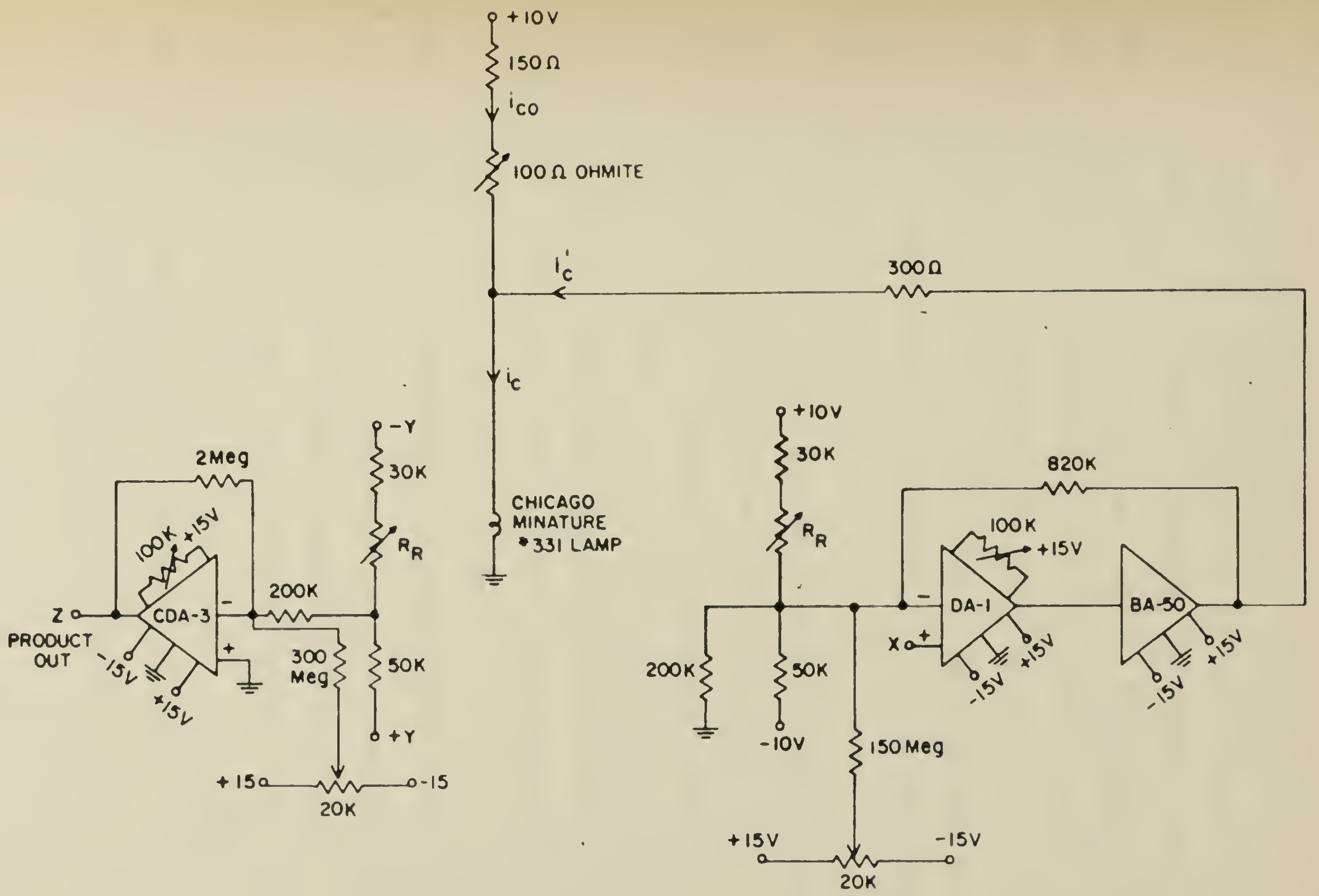

Fig. 5-4: FINAL MULTIPLIER CIRCUIT

the BA-50 output and the lamp is just about the minimum (with safety factor) required for amplifier protection should the lamp burn out.

Figure 5-5 consists of the plots for the products $Z = X$, $Z = \frac{3X}{4}$, $Z = \frac{X}{2}$, and $Z = \frac{X}{4}$. In the figure, Z was plotted against $10X$ where X took on values from -1.0 volts to +1.0 volts in .2 volt steps. As the data shows an additional gain of 1.169 is needed on the output stage because the gain of the multiplier itself is not unity in the case where $Z = X$. In these tests, the maximum error was 0.62 per cent of full scale. This was calculated by using the slope of the $Z = X$ product to compute the ideal values of Z for all four cases. Full scale was 20 volts (±10 volts).

The results of the dynamic tests were better than those obtained previously. Product distortion became noticeable at about 4 cps. Figures 5-6(a), (b), and (c) show the product Z superimposed on $10X$, where X was a 2 volt peak to peak sine wave, for frequencies of 2.5, 3.0, and 4.0 cps respectively. Appreciable distortion of the product at 5.0 cps is shown in Fig. 5-6(d), a trace of Z alone. In Fig. 4-10, it was noted that the amplifier output showed traces of temporary oscillations at frequencies higher than 2.75 cps. The amplifier finally saturated at just over 3.5 cps. At that time it was hypothesized that these oscillations may have been caused by the high gain of the feedback loop when R_R was at its low value of $R_{RL} = 20K$. The Thevenin equivalent input resistance in that case, with $R_1 = 36K$, was 12.86K giving a gain of $\frac{820K}{12.86} \approx 63$. Figures 5-6(e), (f) and (g) the output of the BA-50 at 2.5, 3.5, and 4.0 cps respectively show slight oscillations beginning at 3.5 cps. However,

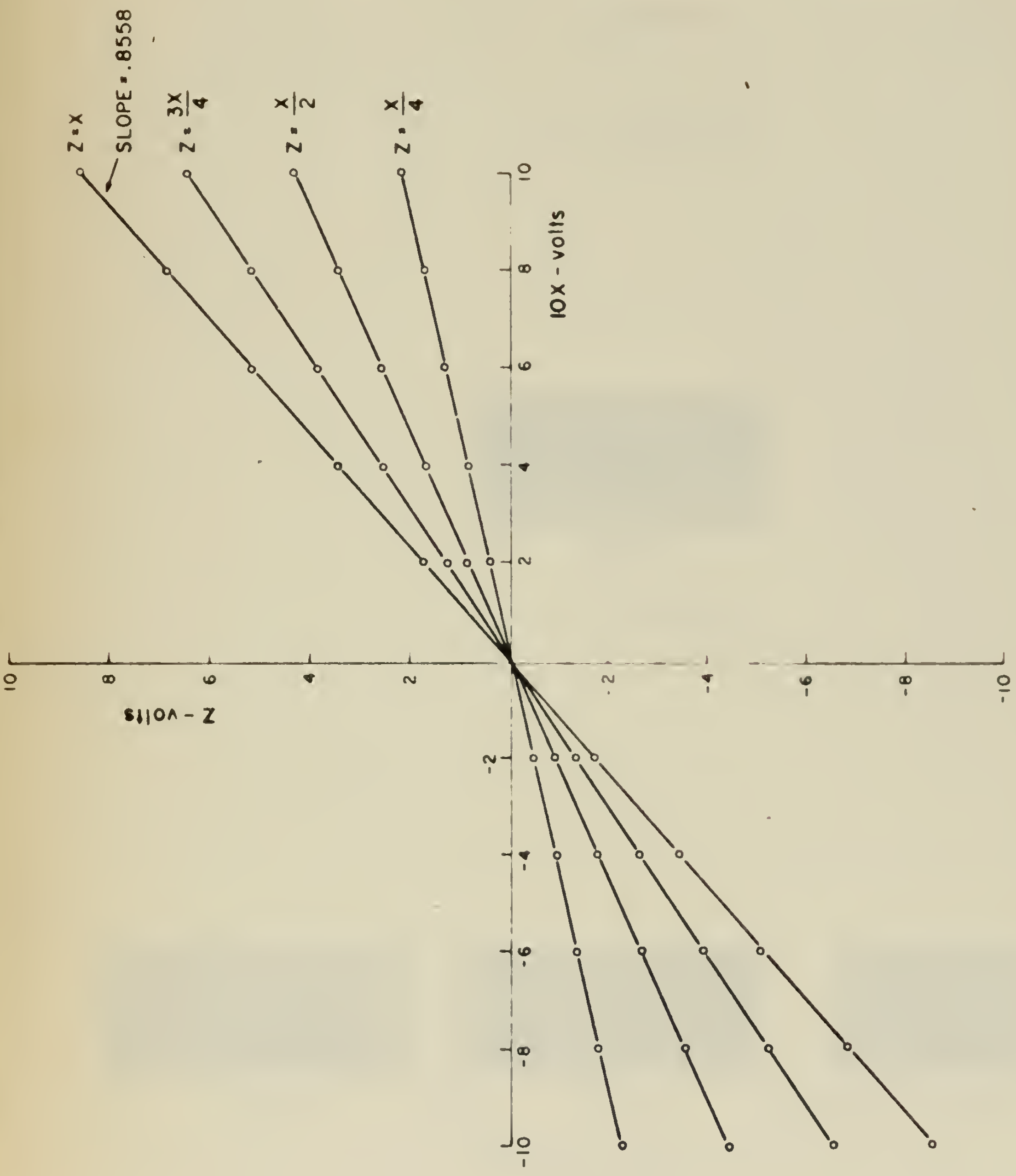

Fig. 5-5 PRODUCT PLOTS Z vs 10X

(a) 2.5 cps
0.2 sec /cm

(b) 3.0 cps
0.1 sec / cm

(c) 4.0 cps
0.1 sec /cm

X - 1 volt /cm
Z - 10 volts / cm

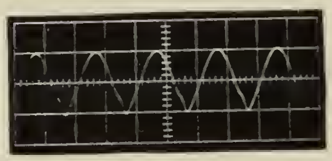

(d) 5.0 cps
0.1 sec / cm

Z - 10 volts/cm

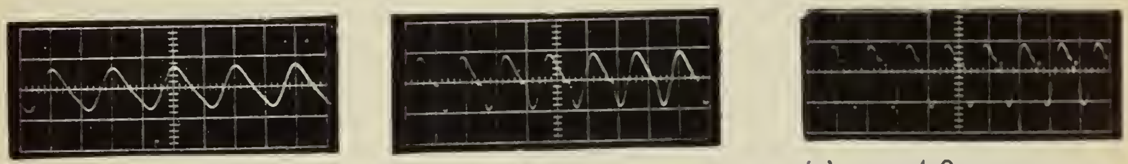

(e) 2.5 cps

(f) 3.5 cps

(g) 4.0 cps

Amplifier Output
0.2 sec / cm
5 volts / cm

Fig. 5-6: SCOPE PHOTOS

in none of these instances does the amplifier output exceed ±5 volts. For comparison, the Thevenin equivalent resistance for the feedback loop with R_R at its low value of 11K is 22.5 K with less than half the equivalent voltage, i.e 1.0 volts compared to 2.5 volts before. The gain in this case is $\frac{820K}{22.5K} \approx 36$. This seems to at least partially explain the improvement of frequency response.

CHAPTER VI

CONCLUSIONS AND RECOMMENDATIONS FURTHER DEVELOPMENT

The Analog Electro-Optical Multiplier satisfied the design requirements of 1 per cent accuracy and 2 cps or better dynamic range with .62 per cent accuracy and a 4 cps frequency limit on X. There is little doubt in the author's mind that these figures can be improved upon. One might try experiments with different voltage divider configurations in order to further limit the effects of voltage sensitivity, which is believed to be the major source of error. Frequency response might be improved by using a faster lamp. It has been suggested that electroluminescent panels might be adapted for use as a light source. They are not directly applicable because they operate on a-c, require high voltage (low current however), and their light output depends upon the frequency of the input. Modulation techniques of some sort, however, might permit their use in this multiplier. Their advantages would be the increased speed of response and the good degree of light uniformity without using diffusing apparatus.

In order to build a number of these multipliers which work well, one must be very careful in choosing the photoconductive cells. If a type of cell which is less sensitive to voltage can be obtained while maintaining the temperature and hysteresis characteristics of the CdS, these should also be tried. At any rate, choosing the cells

which are to be grouped in one photocell package with a single master may require a certain amount of trial and error to find those which can be matched by means of the allowed adjustment range. Inability to obtain the use of an oven forestalled the conducting of extensive temperature tests, and this is still another area for investigation.

An immediate task is to submit a proposal for the construction of still another lamp-photocell package. Figure 6-1 incorporates those features which the author deems necessary for success. The proposed design should enable the uniform illumination of all eight cells. Although some space has been left on either side of the group of photocells to lessen any possible shadowing effects from the corners, the overall width dimension has been reduced. If the wall of the chamber containing the lamp is spaced at 1 1/2" from that containing the cells, this should be sufficient with provision for moving the lamp in and out for fine adjustment as well as replacement purposes. The photocell adjustment range might be increased slightly to allow for correction of a greater amount of mismatch or non-uniform illumination. The material used for the diffuser between lamp and cells is still another variable although the presently used plastic seems to be adequate. The overall simplicity and the acceptable results attained thus far with this multiplier warrant further investigation and development.

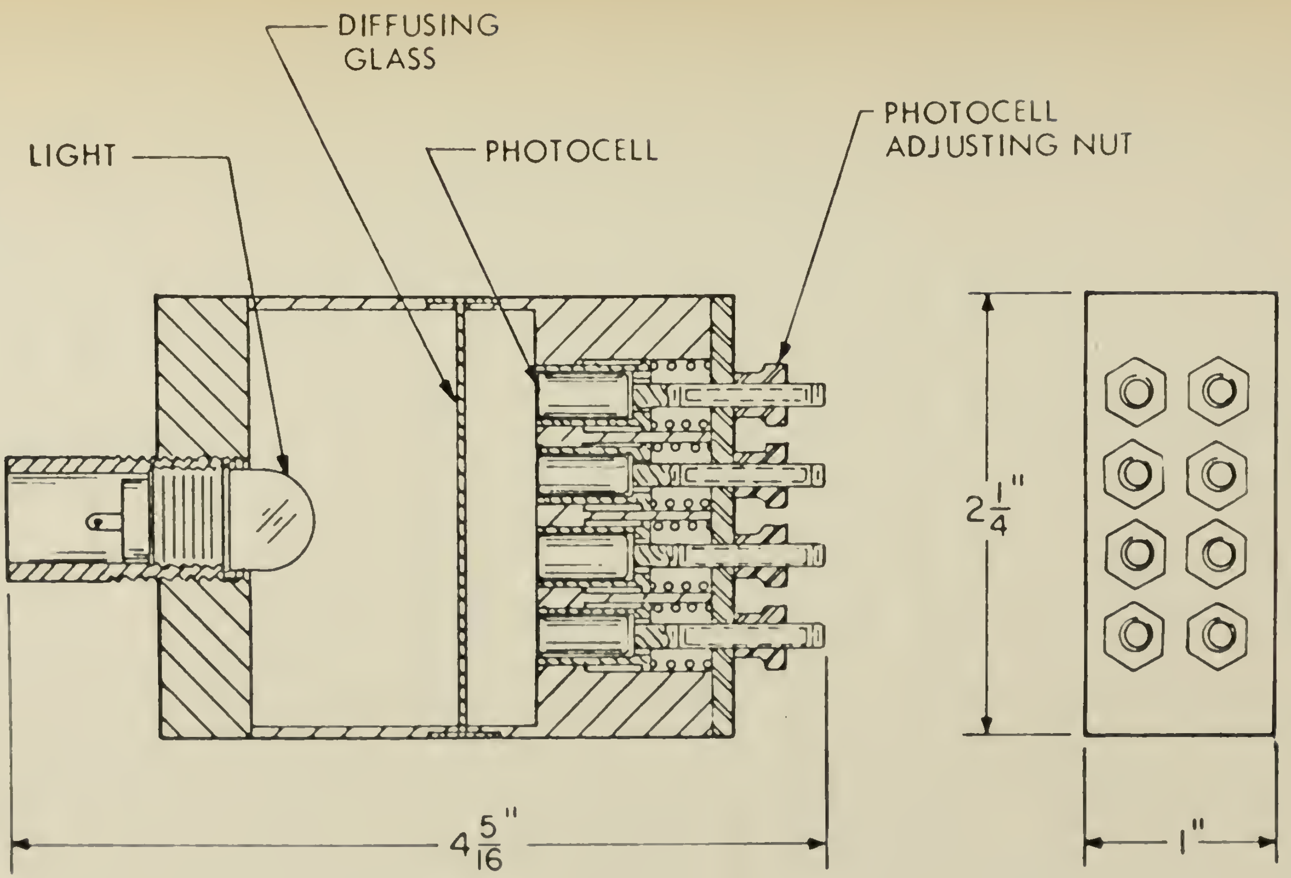

Fig. 6-1 PROPOSED LAMP-PHOTOCELL PACKAGE

APPENDIX I

Hysteresis, signal heating, and signal voltage all seem to affect the resistance of the photocell in the Raysistor to a noticeable extent. Figure A-1 gives the experimental set-up used for hysteresis measurements. By opening and closing the switch, we were able to switch back and forth between two values of R_R which were determined by settings on the 100 Ω and 2500 Ω pots. With the switch open the 100 Ω pot was adjusted to obtain the initial value of R_R for the particular test. The 100 K pot was then used to zero the meter reading. Then the switch was closed, causing an immediate change in V_c and therefore R_R. The amount of change was dictated by the setting on the 2500 Ω pot. The switch was opened again after one minute returning V_c to its initial value. The deflection from null was recorded and observations were made on the time required to reassume either the null or a steady state condition. In general the results showed that the hysteresis effects were increased as R_R was increased. Switching from an initial value of R_R to some lower value and back again to the initial value almost always resulted in fairly rapid return to null. However, switching from the initial value to a higher value and back again resulted in eventual steadying at a voltage offset from null. Typical results are given in Fig. A-2. In the table shown, R_{Ri} is the initial value of R_{Ri}, R_{Rt} is the temporary value obtained by switching, and the initial offset is the voltage offset from null recorded immediately after opening the switch.

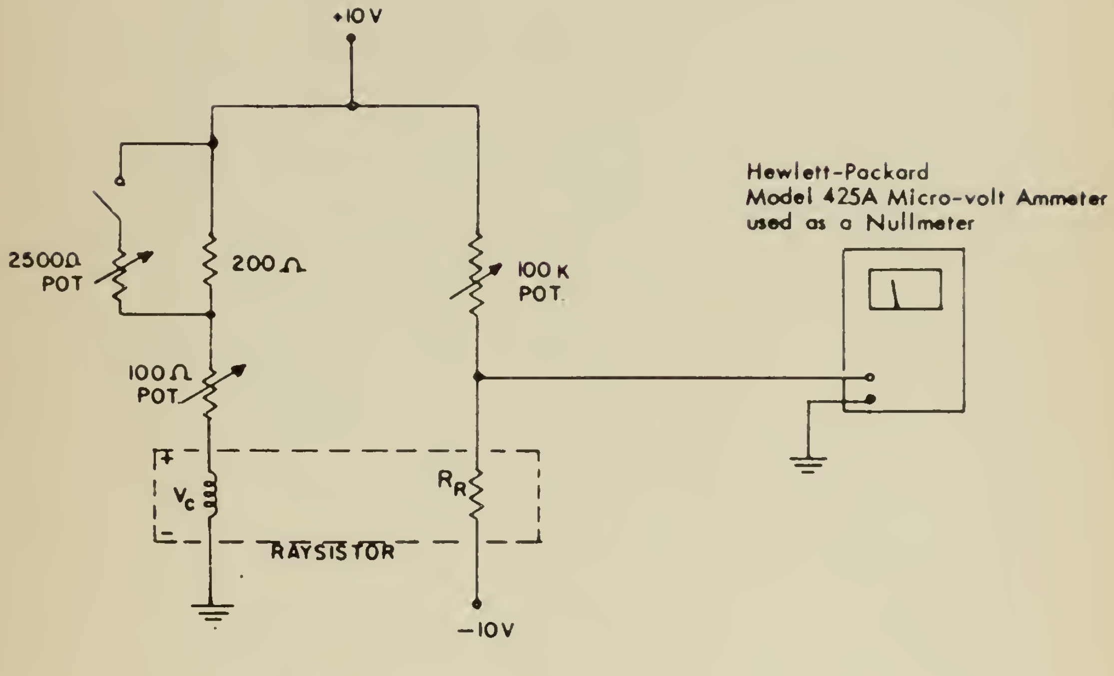

Fig. A-1: EXPERIMENTAL SET-UP FOR HYSTERESIS MEASUREMENTS

R_{Ri}	R_{Rt}	Initial Offset	Final Observations
2K	1K	-.03 volts	Return to null in 30 secs.
2K	4.5K	-.07 volts	Steady at -.04 volts after 3 mins.
27K	2K	-.26 volts	Return to null in 30 secs.
27K	100K	-.08 volts	Steady at -.07 volts after 3 mins.

Figure A-2

Figure A-3 gives plots of the i-v characteristics for a Raysistor. The data was obtained by fixing the voltage across the lamp and varying the voltage across R_R from 1.02 volts to 10 volts in 1 volt steps, reading the current through the photocell at each step with the Hewlett Packard 425A used as an ammeter. The plots show that either signal voltage or signal heating effects were evident once the voltage across the photocell exceeded 4 volts. The same experiments with the CdS photocells which were used in the later design of the multiplier resulted in the i-v characteristics shown in Fig. A-4. By comparison, these cells were not affected by signal heating or signal voltage to as great an extent.

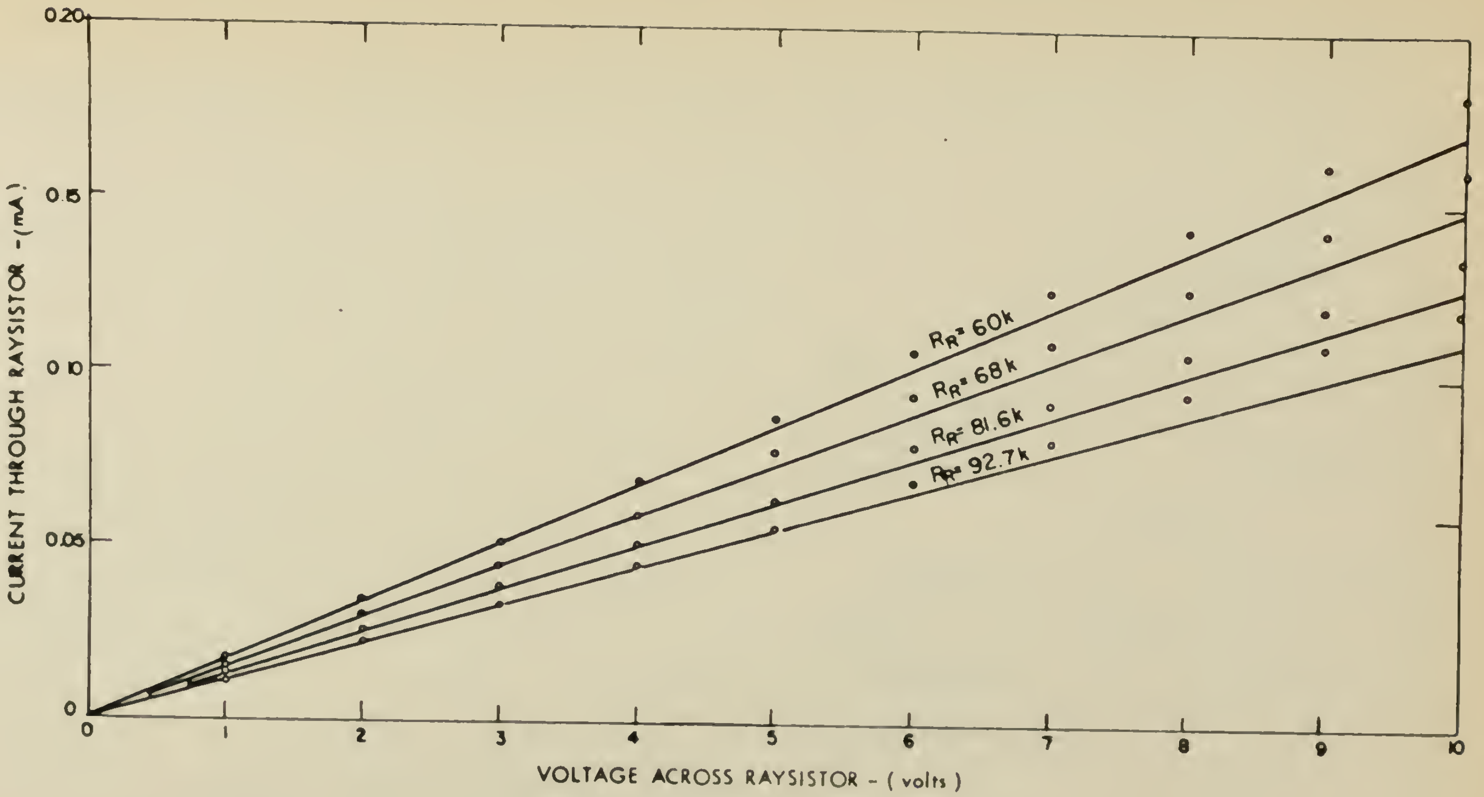

Fig. A-3: RAYSISTOR i-v CHARACTERISTICS

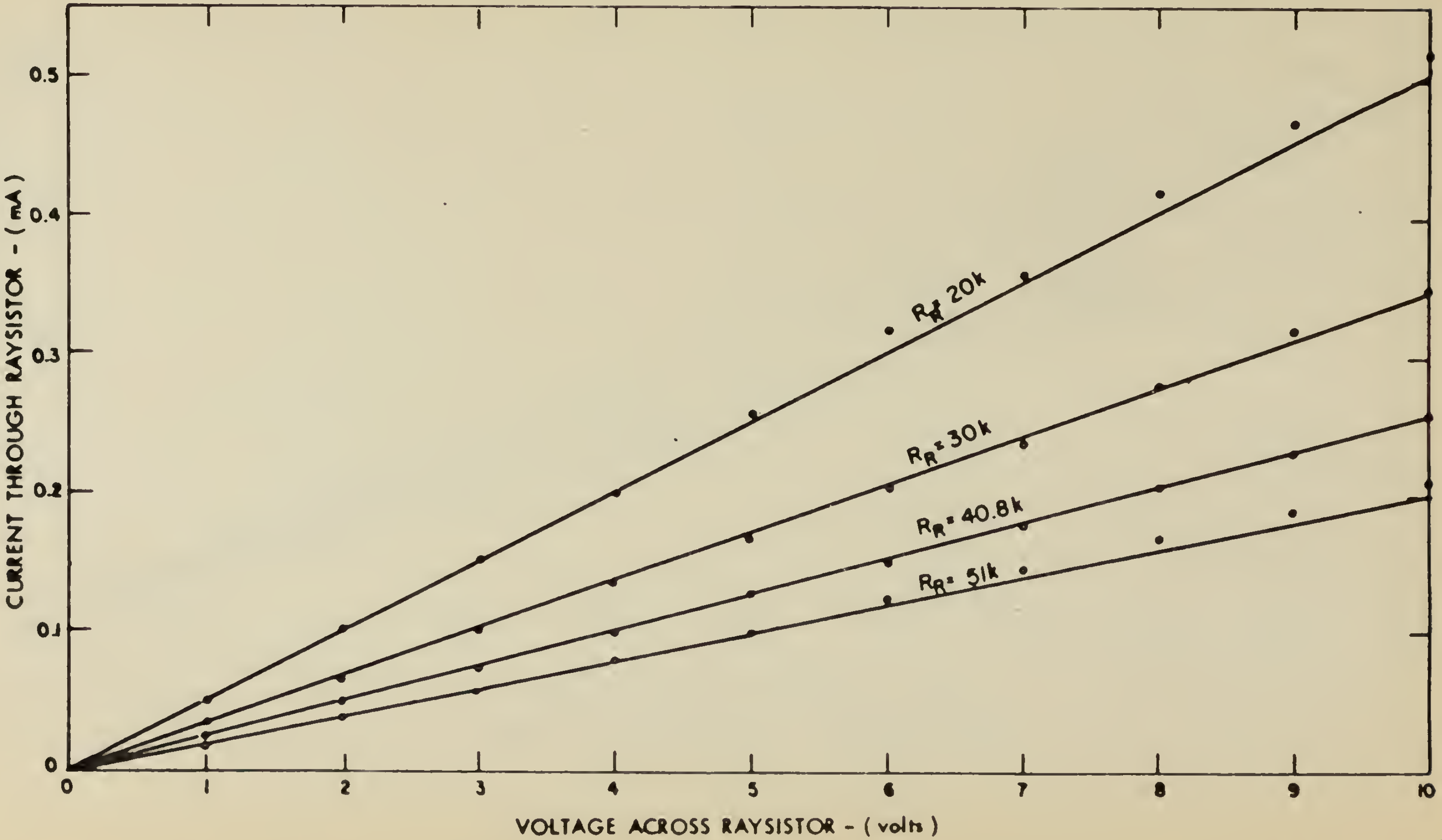

Fig. A-3a Raysistor i-v Characteristics (cont'd)

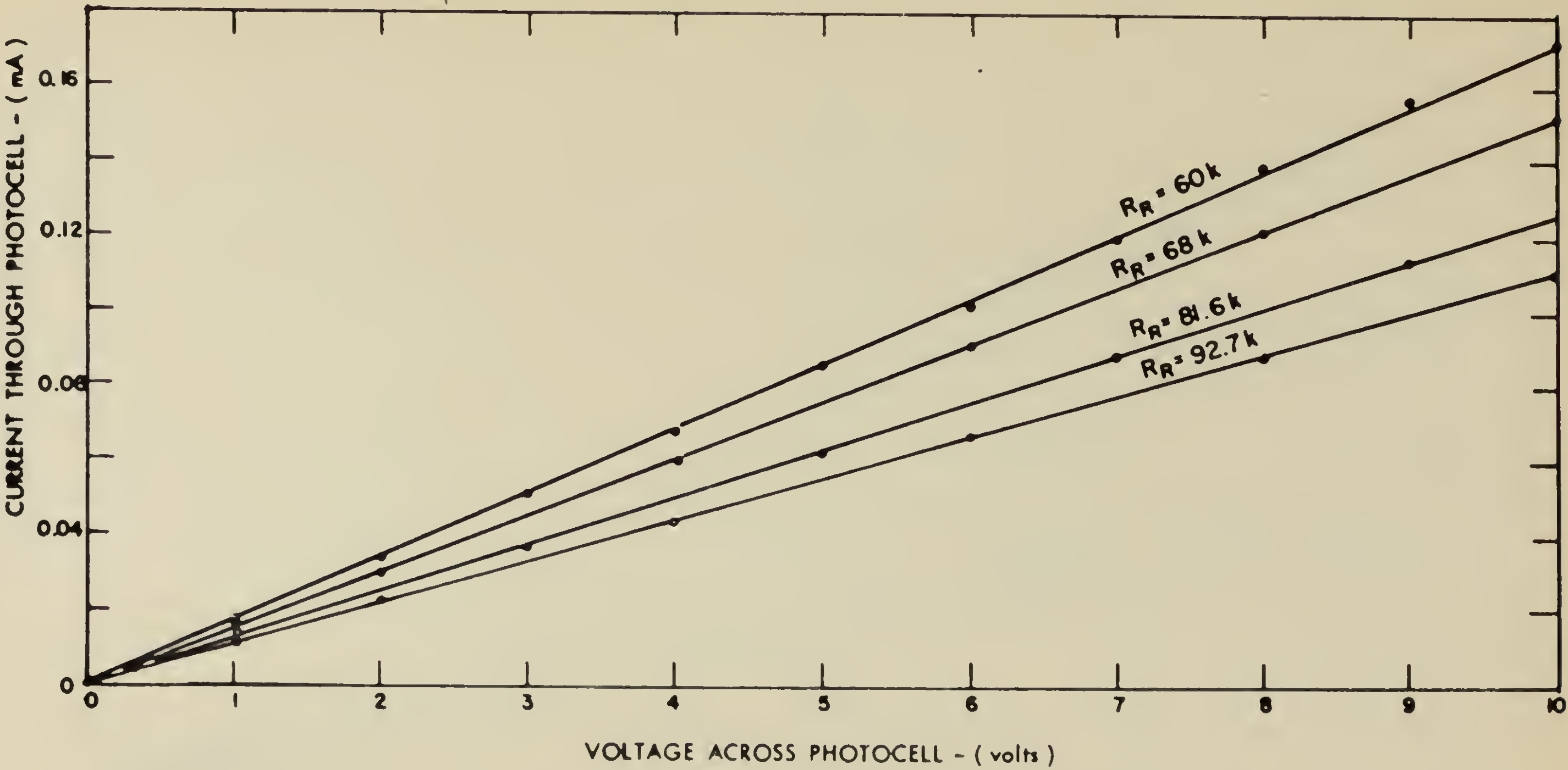

Fig. A-4: Cds PHOTOCELL i-v CHARACTERISTICS

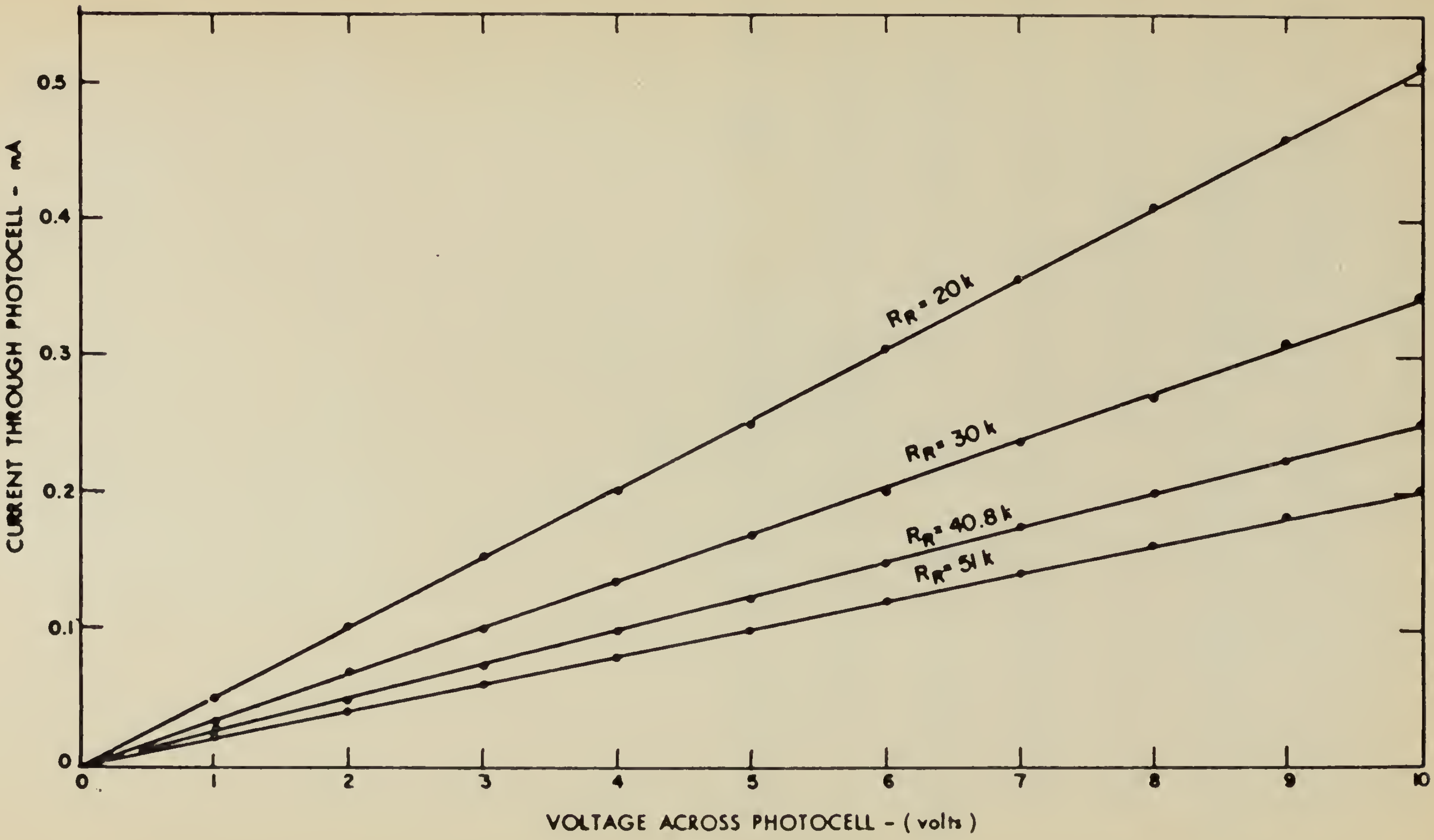

Fig. A-4a: Cds Photocell i-v Characteristics (cont'd)

BIBLIOGRAPHY

1. Korn, G. A. and Korn, T. M., Electronic Analog Computers, 2nd Edition, McGraw-Hill, New York, 1956.

2. Solbakken, A., "Four-Quadrant Analog Multipliers," Massachusetts Institute of Technology, Electronic Systems Laboratory, D. S. R. Project 8823, Memorandum 2, September 28, 1962.

3. Nexus Research Laboratory, Dedham, Massachusetts, Short-Form Catalog, Bulletin A-TB-2.

4. Raytheon Company, Industrial Components Division, Newton, Massachusetts, Product Data CK1102, CK1103, CK1104, CK1112, June 15, 1961.

5. Clairex Corporation, New York, N. Y., "Clairex Photoconductive Cells," Publication 100CL363A.

6. Nexus Research Laboratory, Dedham, Massachusetts, Application Note APP-1b, October 1962.

7. Zemansky, Mark W., Heat and Thermodynamics, McGraw-Hill, New York, 1957.

MASSACHUSETTS INSTITUTE OF TECHNOLOGY
1861